# $NO_x$ Depolluting Performance of Photocatalytic Materials in an Urban Area – Part I: Monitoring ambient impact

**Jaime Fernández-Pampillón [a, b,*], Magdalena Palacios [b], Lourdes Núñez [b], Manuel Pujadas [b], Beatriz Sanchez [c, b], Jose Luis Santiago [b] , Alberto Martilli [b]**

[a] The National Distance Education University (UNED), Madrid, Spain
[b] Research Centre for Energy, Environment and Technology (CIEMAT), Madrid, Spain
[c] Department of Geography, National University of Singapore, Singapore

*Corresponding author: Jaime Fernández-Pampillón; Email address: Jaime.Fernandez@ciemat.es

## ABSTRACT

In the framework of the LIFE MINO$_x$-STREET European project (co-financed by the EU), a commercial photocatalytic product consisting of a $TiO_2$-based water solution was selected to be implemented and tested on the bituminous asphalt of a main road of the Municipality of Alcobendas (Madrid, Spain), covering an area of approximately one thousand square meters both ways. This coating material was selected after rigorous laboratory assays of a variety of commercial photocatalytic products.

An expressly-designed experimental system has allowed to evaluate during 41-days the $NO_x$ depolluting ability of the photocatalytic material in that urban scenario. $NO_x$ ambient concentrations were monitored at several points located along the longitudinal axis of the selected road, both inside and outside the treated area with photocatalytic material. Moreover, meteorological and ambient parameters at building's roof height were monitored to document the boundary conditions in the experimental area.

In spite of the selected photocatalytic material showed a remarkable surface deposition velocity (7.2 $10^{-3}$ m $s^{-1}$) in laboratory tests and although the experimental deployment has been carefully designed and implemented to robustly compare control and test scenarios with a high time and spatial resolution, when analyzing average $NO_x$ concentrations under filtered optimal ambient conditions to guarantee the photocatalytic effect to be maximum, no clear trend could be observed in the ambient $NO_x$ concentrations that could be unequivocally associated with the sink effect induced by the implemented photocatalytic material.

The results have shown that the $NO_x$ gradients formed along the road were quite large even without photocatalytic coating, reflecting a complex atmospheric reality far from a homogeneous behavior along the street, which made extremely difficult to observe the weak $NO_x$ sink effect existing. In fact, taking into account the precision of the experimental system, the potential environmental $NO_x$ purification capacity, if it had existed, would have had to be greater than 3% to be observed under the experimental conditions. This finding agrees with the estimates made by means of a simple but consistent first-order kinetic calculation for which an environmental reduction of $NO_x$ of less than 1% was obtained.

All the collected data have given detailed valuable information for evaluating the results provided by a mathematical model capable of simulating the dispersion of air pollutants at urban street scale. As it is presented in the Part II of this study, these simulations permitted to estimate accurately the

impact on air quality of the use of this remediation technology not only under the actual experimental conditions but also in other urban scenarios.

**KEYWORDS**

Air pollution, photocatalytic bituminous pavement, $TiO_2$, $NO_x$ remediation, real scale demonstration

## INTRODUCTION

Air pollution is the single largest environmental issue that affects public health globally. Experimental and epidemiological studies continue to accumulate evidence on the association between different serious effects on health, such as premature mortality and morbidity, mainly related to cardiovascular and respiratory disorders, and exposure to different atmospheric pollutants [WHO Regional Office for Europe, 2017].

In particular, WHO and literature reviews have shown that short-term exposure to nitrogen dioxide ($NO_2$) increases respiratory hospital admissions and some support also exists for all-cause mortality while more robust long-term effects appear associated to bronchitis symptoms in asthmatic children [Samoli et al., 2006; WHO Regional Office for Europe, 2013]. For example, according to the European Environmental Agency, 68000 premature deaths were attributed to $NO_2$ exposure in the EU-28 in 2016 [European Environment Agency, 2019 a].

The road transport sector continues to be the source that contributes the highest proportion of nitrogen oxides ($NO_x = NO + NO_2$) emissions to the atmosphere (39% in the EU-28 in 2017) [European Environment Agency, 2019 a]. During the last two decades, Europe has applied very strict measures to improve air quality and comply with the EU limits of the air quality standards [Directive 2008/50/EC of the European Parliament and of the Council of 21 May 2008 on ambient air quality and cleaner air for Europe, 2008], having achieved a reduction in $NO_x$ emissions, for the period 1990-2017, for all the sectors as a whole of around 57% and being this reduction even greater for the road traffic sector (close to 61%) [European Environment Agency, 2019 b].

Despite these efforts, the limit values for $NO_2$ ambient concentrations continue to be exceeded, especially in urban environments. In fact, while overall $NO_x$ emissions from road traffic decreased noticeably, 10% of all stations in EEA-39 countries registered environmental concentrations above the annual limit value in 2017, being widely distributed throughout Europe. The 98% of all values above this threshold were observed in urban or suburban areas. In addition, concentrations above the hourly limit value were observed mainly at urban traffic stations [European Environment Agency, 2019 a].

This situation is partly due to the growth in the use of diesel vehicles and the increase in the proportion of $NO_2/NO_x$ emissions since the implementation of the Euro 3 Diesel Oxidation Catalyst technology [Carslaw et al., 2016]; other studies have shown that the reduction of primary $NO_2$ emissions might not have a noticeable influence on urban $NO_2$ concentrations and only a substantial reduction of local $NO_x$ emissions could help to meet the $NO_2$ limits [Kurtenbach et al., 2012].

On the other hand, the United Nations foresee an increase of the European urban population during the period of 2015 to 2050 of 9.8 percentage points, reaching 84% of the total European population. This circumstance, together with the possible breach of the limit values of $NO_2$, would imply an important increase in exposure to $NO_2$ in great European urban areas. This is the case of Madrid area (Spain) where the city and other densely populated agglomerations of the region frequently exceed the hourly and annual limits for $NO_2$ [Ayuntamiento de Madrid, 2017; MAPAMA, 2017; United Nations, 2018].

In order to reduce the contribution of $NO_x$ to air pollution in urban areas, different mitigation strategies are being implemented and evaluated. One of the emerging environmental control options with potential success in the removal of air pollutants is the use of building materials that incorporate photocatalytic compounds such as titanium dioxide ($TiO_2$) which, activated by sunlight, allow the elimination of pollutants such as $NO_x$ from the air through heterogeneous photocatalysis [Chen et al., 2012]. This technology has had a remarkable development and has led to the commercialization of a number of photocatalytic products in which $TiO_2$ is a component of paints or coatings as well as a constituent element of the construction material itself, founding in the European urban environments a huge field of application for depolluting purposes.

In numerous tests developed at laboratory scale in last decade, carried out under different experimental conditions, an efficient reduction of $NO_x$ on photocatalytic surfaces is generally observed [Ballari et al., 2010; Laufs et al., 2010; Martínez et al., 2011; de Melo and Trichês, 2012; Ângelo et al., 2014; Mendoza et al., 2015; Sikkema et al., 2015; Zouzelka and Rathousky, 2017; Mothes et al., 2018] and most of these studies concluded that $NO_x$ are converted to nitrate, that remains adsorbed on the photocatalytic surface and could be subsequently removed by washing [Bengtsson and Castellote, 2010; Laufs et al., 2010; Martínez et al., 2011; Karapati et al., 2014].

On the other hand, several field experimental studies have been developed at real scale in outdoor conditions whose results concerning the reported efficiency of $NO_x$ reduction on treated surfaces are dissimilar, from high $NO_x$ remediation (19 to 80%) [Guerrini and Peccati, 2007; Maggos et al., 2008; Chen and Chu, 2011; Ballari and Brouwers et al., 2013; Boonen and Beeldens, 2014] to low or non-detectable reduction [IPL, 2010; Gallus et al., 2015 a; Gallus et al., 2015 b; Tremper and Green, 2016]. Such a controversial outcomes could have their explanation on several factors as ambient experimental conditions (meteorology and air quality), urban morphology of the studied site or the characteristics of the different photocatalytic products applied on distinct substrates. In fact, the interaction between atmosphere and urban surfaces involves processes at different spatial and temporal scales inducing complex flow patterns and strong gradients of pollutant concentration within the urban canopy, making it difficult the characterization of pollutants distribution.

The research question that motivates this work is then: How to experimentally quantify the potential reduction in $NO_x$ ambient concentration due to the implementation of photocatalytic materials in a real street located in a medium density urban neighbourhood?

To answer this question and having in mind the experiences mentioned above, a robust design of the field experiment seems to be crucial to study if changes detected in ambient pollutant concentrations are related to the presence of photocatalytic surfaces in the scenario of interest or are due to other factors [Department for Environment Food and Rural Affairs, 2016]. Additionally, after any exhaustive experimental field study, an adequate modelling of the urban scenario at microscale would be appropriate to quantify the contribution of the different factors potentially related to the possible observed sink effect on $NO_x$. Therefore, studies under realistic environmental conditions are necessary to better estimate the real potential impact on ambient $NO_x$ concentrations of the use of photocatalytic products in urban areas.

Research on the application of photoactive building materials is mostly limited to sidewalk pavements or facades, being very scarce those studies devoted to the impact that they could have on urban ambient air when are used as coating on asphalt pavements [Ballari et al., 2011; Hassan et al., 2013; Boonen and Beeldens, 2014]. In this work we specifically present the results of studying the effect of the use of a selected photocatalytic coating, designed to be applied in bituminous mixtures, on the environmental levels of $NO_x$ in a true urban canyon in the city of Alcobendas, which is a novelty with respect to the studies developed so far.

The work presented in this contribution has been done in the framework of the LIFE MINO$_x$-STREET project (Monitoring and modelling $NO_x$ removal efficiency of photocatalytic materials: a strategy for urban air quality management) [LIFE MINO$_x$-STREET, 2020], co-financed by the LIFE Financial Instrument of the European Union and executed from July 2013 to July 2018, that was conceived as a demonstration project whose main objective has been to test the real capacities of different commercial photocatalytic materials to reduce urban atmospheric $NO_x$ concentrations. With this purpose, a variety of commercial $TiO_2$ based photocatalytic building materials have been subjected to rigorous laboratory assays in order to study, on one hand, their mechanical and physical properties [Cadavid et al., 2015], operation-induced changes and durability [Palacios et al., 2015 a] and, on the other, their photoactivation and air-purifying capacity [Palacios et al., 2015 b; Palacios et al., 2015 c] and chemical and structural properties as well as the changes induced by ageing and regeneration processes [Sánchez et al., 2014; Sánchez et al., 2015; Suárez et al., 2017]. Moreover, the identification and quantification of some possible by-products generated that may have harmful effects on public health have been accomplished [Núñez et al., 2018].

Then, the most promising materials were selected and assayed by means of both outdoor experiments [Palacios et al., 2015 d] and controlled assays under ambient conditions [Palacios et al., 2015 e]. Additionally, three different photoactive products were selected based on rigorous laboratory tests. These materials were implemented in three urban scenarios in the city of Alcobendas, in the Madrid region (Spain) and measurement campaigns were carried out in each scenario: real street-canyon (roadway scenario), artificial street-canyon (sidewalk and facade scenarios). For this purpose, several experimental systems, specifically adapted to each case, were designed and arranged to try to establish a causal relationship between the presence of photocatalytic material implemented in each scenario and a possible observable decrease in $NO_x$ concentrations in the air.

## EXPERIMENTAL

### Street canyon field site

This kind of outdoor experiments, defined to test the ambient depolluting efficiency of photocatalytic materials, require the choice of the appropriate scenario. In this case, to test the chosen photoactive material to be used on roadway the selection of a suitable street was crucial and it was conditioned by several factors: a) the necessity of an existing asphaltic mixture compatible with the chosen photocatalytic coating material; b) the convenience that the scenario was a straight street-canyon with a height/width ratio close to 0.5 to guarantee sufficient ultraviolet radiation on the road for the photocatalytic phenomenon to take place during several hours around noon; c) that the test area registered moderate daily mean traffic intensity; d) a minimum infrastructure to allow the implementation of the measuring system deployment.

Attending all these requirements, the selected urban scenario was a stretch of the Paseo de la Chopera, a main street of the Municipality of Alcobendas (located 10 km NE of Madrid city and with more than 117.000 inhabitants). This street is 300 m long x 36 m wide, with buildings around 16 m height, bounded by roundabouts at both ends and its road consists of two lanes in each traffic direction and a median strip.

A section of 60 m long, located approximately in the centre, was selected to be covered with the photocatalytic coating, applied over a width of around 16 m, covering the road and the median strip but not the sidewalks (see Figure 1). The length of the photoactive zone was considered adequate to be able to observe a possible $NO_x$ sink effect since it had previously been observed in an experimental system implemented in a 15 m diameter photocatalytic platform installed in a suburban area of Madrid [Palacios et al., 2015 d]. Moreover, the East-West orientation of the street (273 degrees) allowed a large part of the road to receive direct solar radiation during the potentially photoactive daytime period of the campaign.


**Figure 1**. Experimental area, Paseo de la Chopera (Alcobendas). Locations of sampling points during the measurement pre-campaign (represented by the square, P0) and the experimental campaign (represented by the dots, P1 to P7).

**Photocatalytic material**

The selected photocatalytic coating consisted of a water emulsion with a suspension mainly composed of $TiO_2$. This product was selected among various due to its good NO depolluting efficiency obtained in laboratory assays under the ISO 22197-1:2007 international standard method, designed for testing the air-purification performance of semiconducting photocatalytic materials, specifically the removal of nitric oxide [ISO, 2007]. This procedure is based on the use of a little photoreactor where a sample of the photoactive material of interest in flat sheet is UVA irradiated (simulating the effect of solar radiation) under the presence of a controlled gas flow enriched in NO. After 5 h of exposing the sample under those conditions, the ratio between $NO_x$ inlet and outlet concentrations in the photoreactor gives the information for evaluating the photocatalytic activity and the depolluting efficiency of the photoactive sample. In this case the NO removal efficiency was 55% for an NO average inlet concentration of 0,997 ppm. Modified-ISO laboratory assays in which NO averaged inlet concentration was set to 530, 265 and 140 ppb, revealed no change in resulting abatements. Additionally, an estimate of NO surface deposition velocity for this material was obtained for the latest test conditions. At that concentration, in the range of atmospheric relevant pollution levels, a classical first-order kinetic approximation was used [Ifang et al., 2014; Mothes et al., 2018], giving a result for NO surface deposition velocity of 7.2 $10^{-3}$ m $s^{-1}$. Interestingly, activity was similar to those obtained for NO by other studies [Gallus et al., 2015 a; Ifang et al., 2014; Engel et al., 2015; Mothes et al., 2018]. Nevertheless, it is important having in mind that in such ISO bed photo-reactors, transport limitations occur that can lead to underestimation of the activity by possible diffusion limitations (Ifang et al., 2014).

On the other hand, in this work no estimates have been made of the surface deposition rates of $NO_2$. However, laboratory experiments carried out with several $TiO_2$-based photocatalytic materials have given values of the same magnitude or lower than that obtained for NO [Ifang et al., 2014; Engel et al., 2015; Gallus et al., 2015 b; Department for Environment Food and Rural Affairs, 2016; Mothes et al., 2018].

Typically, models describe deposition process through a three-terms resistance scheme that takes into account the following factors: the surface activity that is included through the surface deposition velocity estimated from laboratory assays, the turbulent mixing and the quasi- molecular diffusion. This overall deposition velocity, that also can be estimated from field experiments in ambient air (Palacios et al., 2015 d), is always lower than the surface deposition velocity.

**Experimental set up**

Firstly, in order to characterize the air quality at a location near the studied street minimally affected by the nearby urban morphology, a pre-campaign was carried out from November $3^{rd}$, 2014 to January $1^{st}$, 2015. Meteorological instrumentation and gas analysers (Table 1) were installed inside a mobile unit (P0) (Figure 1) with that purpose.

The campaign itself to document the ambient effect of applying the photocatalytic coating in Paseo de la Chopera was operative from $12^{th}$ September to $22^{nd}$ October, 2015. The experimental system was designed to monitor the air quality and meteorological parameters in different points of this scenario (see Figure 1 and Table 1). During the first two weeks, that is, before the implementation of the photocatalytic coating, the system was monitoring this scenario to obtain background information.

The photocatalytic coating was applied on September $23^{rd}$ and $24^{th}$, 2015. The product was implemented spraying the water emulsion on the bituminous pavement by means a distributor truck with a spray bar with nozzles fitted on the back. The application was done on a central section of the road, including the median strip, so that along the chosen street there were three consecutive zones: conventional roadway-photocatalytic roadway-conventional roadway.

After applying this coating, the photocatalytic activity of the resultant photoactive bituminous pavement was tested periodically. A coring of the asphalt mix of two test sections (side and centre) was carried out and the samples obtained were cut into small adapted specimens so that the photocatalytic activity of these concrete samples could be tested under the mentioned ISO standard.

In urban areas, the spatial variability of air pollutant concentration is very strong as a result of the complex air flows due to the buildings or other obstacles that promote the development of strong gradients in the pollutant concentrations (Vardoulakis et al., 2003, 2011 a, 2011 b; Buccolieri et al., 2011; Amorim et al., 2013; Vos et al., 2013; Gromke and Blocken, 2015; Borge et al., 2016; Jeanjean et al., 2017; Sanchez et al., 2017; Santiago et al., 2017, 2020; Beauchamp et al., 2018; Rivas et al., 2019). Ideally, the three-zone configuration in this street canyon should allow the observation of horizontal $NO_x$ concentration gradients near the road surface induced by the photocatalytic action of the treated area, especially in conditions of wind flow parallel to the east-west axis of the street for the which is expected that the influence of the dynamics on the observed gradients will be minimized and the detection and documentation of the possible $NO_x$ sink effect in the active area versus the untreated area is feasible.

For this purpose, $NO_x$ ambient concentrations (NO and $NO_2$) were monitored along the longitudinal axis of the road (Figure 1) at six different points (P1-P6), two inside (P2, P3) and four outside the treated area with the photocatalytic material. The air sampling lines consisted in perfluoroalkoxy tubing with 0.4 cm inner diameter and 53 m (lines 1 to 4) (Figure 2) and 12 m (lines 5 and 6) long. All the sampling inlets were located at 40 cm high and the air samples were transport to the respective control booths.

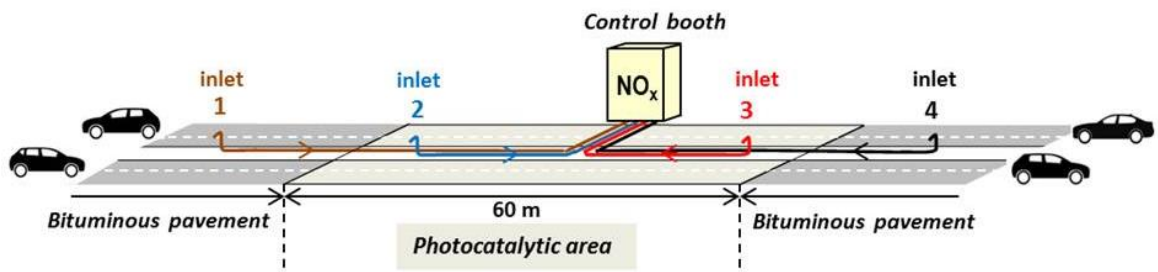


**Figure 2.** Schematic overview of the experimental set up in the central test area of the Paseo de la Chopera (sampling points P1 to P4). Air samples are taken to the $NO_x$ analyser located inside the booth through underground Teflon tubes.

The lines were properly protected and buried under the asphalt surface to prevent damage from road traffic and the action of solar light on the gas samples. Inlet sampling points were located in the middle of the road and protected with meshed cages anchored to the pavement. Particulate filters (cut-off diameter of 15 μm) were placed at the beginning of the sample lines to avoid insects (Figure 3). The sampling height was selected taking into account the results obtained from previous measurements of $NO_x$ concentration vertical gradients over a similar photocatalytic coating in a suburban area [Palacios et al., 2015 d].

**Figure 3.** Photocatalytic stretch of the Paseo de la Chopera. Sampling points P2 and P3 together with the corresponding booth can be distinguished. Details of a meshed cage, a particulate filter at a sampling point and sampling lines before being buried are also shown.

In the central test area, represented in Figure 2, the four lines deliver continuously the air samples to the automatic switching system that sequentially selected each 2 minutes a sample line to be monitored by the $NO_x$ chemiluminescence analyser and the total measurement cycle time lasted 8 min. Only data associated to the second minute of each measurement time of each sampling line were taken into account for $NO_x$ concentration calculation in order to assure that any result could be affected by the measurement correspondent to the previous line. An external pump (3 $m^3$ $h^{-1}$) maintained a constant flow for three of the lines during the time the sampled air mass passing through the fourth line is being analysed. The great advantage of this setup is that using a single analyser allows to remove the possible influence of instrumental uncertainties or possible bias among the $NO_x$ concentrations obtained in each measurement point but the drawback is that the data collection from the four sampling points cannot be simultaneous but sequential.

Additionally, $NO_x$ concentrations were also continuously measured at sampling locations P5 and P6 with 1-minute time resolution by means of two other $NO_x$ analysers located in the respective control booths and data were only used for modelling purposes (Part II of this research) [Sanchez et al., 2021].

As $O_3$ is generally present in ambient air, a change in concentrations could occur due to the reaction of NO with $O_3$ during the transport in the sampling lines or even in the analyser. Unfortunately, no surface ozone measurements were available during the measurement campaign, which is why the error induced by the conversion of NO to $NO_2$ is unknown. Therefore, the results presented using the concentration values of NO and $NO_2$ have served the purpose of a mere qualitative analysis of the atmospheric behaviour of these pollutants in the study area.

The chemiluminescence instruments based on molybdenum converters, that are used for indirect $NO_2$ detection are typically used in monitoring networks although it is well-known that are not selective in the $NO_x$ channels and are affected by positive ($NO_y$) interferences. Nevertheless, it has been demonstrated to have a minor influence on $NO_x$ measurements when they are carried out at the proximity of a $NO_x$ emissions source as road traffic [Kurtenbach et al., 2012; Villena et al., 2012].

Ambient $NO_x$ and $O_3$ concentrations and meteorological parameters (wind speed and direction, air temperature, relative humidity, solar irradiance and pressure) were measured continuously (5-

minutes averaged) at P7 from September, 15$^{th}$ 2015 to October, 22$^{rd}$ 2015. All these data were also essential to impose boundary conditions of the microscale modelling (Part II) [Sanchez et al., 2021].

Table 1 summarizes the instrumentation used in the measurement campaign and its location in the experimental scenario. All the instruments were calibrated before the beginning of the experimental campaign and $NO_x$ and $O_3$ analysers were located in temperature-controlled rooms or booths.

**Table 1**. Instrumentation used in the measurement campaigns and its location in the experimental scenario.

| PARAMETER | INSTRUMENT | MODEL | LOWER DETECTION LIMIT / PRECISION / FLOW RATE | SAMPLING SITE |
|---|---|---|---|---|
| NO, $NO_2$, $NO_X$ | Chemiluminescence analyser | Thermo Scientific 42i | 0.40 ppb $NO_x$<br>±0.4 ppb (500 ppb range)<br>0.6–0.8 LPM | P1, P2, P3, P4 |
| NO, $NO_2$, $NO_X$ | Chemiluminescence analyser | Thermo Scientific 42i | 0.40 ppb $NO_x$<br>±0.4 ppb (500 ppb range)<br>0.6–0.8 LPM | P5 |
| NO, $NO_2$, $NO_X$ | Chemiluminescence analyser | Teledyne API 200 A | 0.4 ppb $NO_x$<br>0.5% of reading<br>0.5 LPM | P6 |
| NO, $NO_2$, $NO_X$ | Chemiluminescence analyser | Teledyne API 200 A | 0.4 ppb $NO_x$<br>0.5% of reading<br>0.5 LPM | P0, P7 |
| $O_3$ | UV absorption analyser | Teledyne API 400 A | < 0.6 ppb $NO_x$<br>0.5% of reading<br>0.8 LPM | P0, P7 |
| Wind direction | Wind vane | Met One 590 | | P0, P7 |
| Wind speed | Cap anemometer | Met One 591 | | P0, P7 |
| Air temperature and relative humidity | Thermistor and thin film polymer capacitor | Met One 083R | | P0, P7 |
| Total solar irradiance | Pyranometer | Met One 595 | | P0, P7 |



Gas analyser instruments were calibrated using cylinder of compressed gases at certified concentrations, with $N_2$ as an inert balance gas (Air Liquide) and the dilution and mixing of the gases were accomplished using a dynamic gas calibrator (Thermo Environmental Instruments, 146C) to produce zero checks and span concentrations that were similar to ambient ranges. This calibrator was equipped with $O_3$ generator based on ultraviolet (UV) radiation that was used to calibrate the Teledyne API 400 A monitor as well as to test the efficiencies of the molybdenum $NO_2$ converters in the $NO_x$ monitors (Thermo Scientific 42i and Teledyne API 200 A).

Traffic volume in the street was also exhaustively determined on three different days throughout the measurement period by using a video camera (September 29$^{th}$; October 15$^{th}$ and 22$^{nd}$). An average of 610±113 vehicles/hour was registered in the Paseo de la Chopera. Traffic counts were analysed by category of vehicles (passenger cars, vans, buses, trucks and motorcycles). Figure 4 shows the daily profile of the average number of vehicles on the Paseo de la Chopera, for which passenger cars category represents 85.3% of the fleet, with 9% vans, 2% buses, 1.6% trucks and 2.1% motorcycles. An average speed of less than 60 km $h^{-1}$ was found for the 90% of the fleet (data was supplied by the Police of the Municipality of Alcobendas).

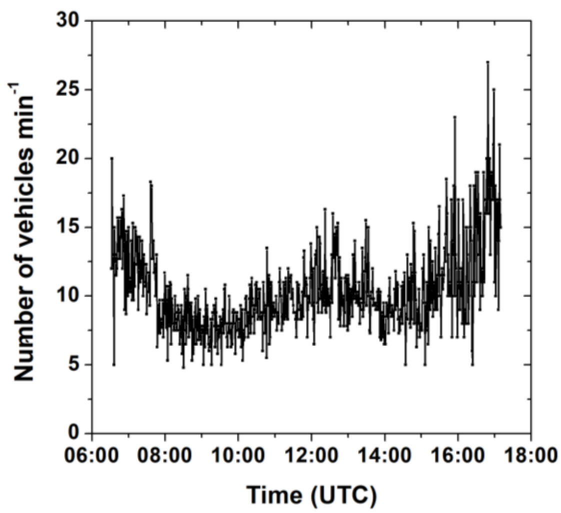


**Figure 4**. Daily profile of the average number of vehicles on the Paseo Chopera for September 29th; October 15th and October 22nd, 2015.

## RESULTS

### $NO_x$ field measurement data

During the pre-campaign phase, the analysis of air quality data recorded at P0 shows a prevalence of Southeast-South-Southwest winds and, occasionally, Northeast in the area during the photoactive daytime periods of the registered episodic situations. In addition, averaged concentrations for NO, $NO_2$ and $O_3$ of 36.2±59.2, 22.8±17.6, 14.6±12.5 ppb were found.

Regarding the experimental campaign itself, the overall $NO_x$ concentration results obtained from the measurements along the road (sampling lines 1 to 4) for control and test scenarios (before and after the application of the photocatalytic coating, respectively) are presented in Figure 5. It is remarkable the importance of fresh vehicle emissions that induces fast changes on the signals making the experimental characterization of the $NO_x$ sink effect potentially generated by the photocatalytic pavement a very difficult task.

The NO and $NO_2$ daily averaged profiles corresponding to the working days of the periods 12th September to 23rd September and 25th September to 22nd October, before and after the application of photocatalytic coating (Figure 6), are clearly associated with the registered traffic pattern at the Paseo de la Chopera (Figure 4). Maximum NO and $NO_2$ concentration values, registered during traffic rush hours, differs noticeably from one measuring point to another and between the analysed periods, especially for $NO_2$ in the late afternoon. During the central hours of the day, the difference is less marked among the sites but also significant, the mean concentration levels for both NO and $NO_2$ being significantly higher during the period after to the implementation of the photocatalytic product.

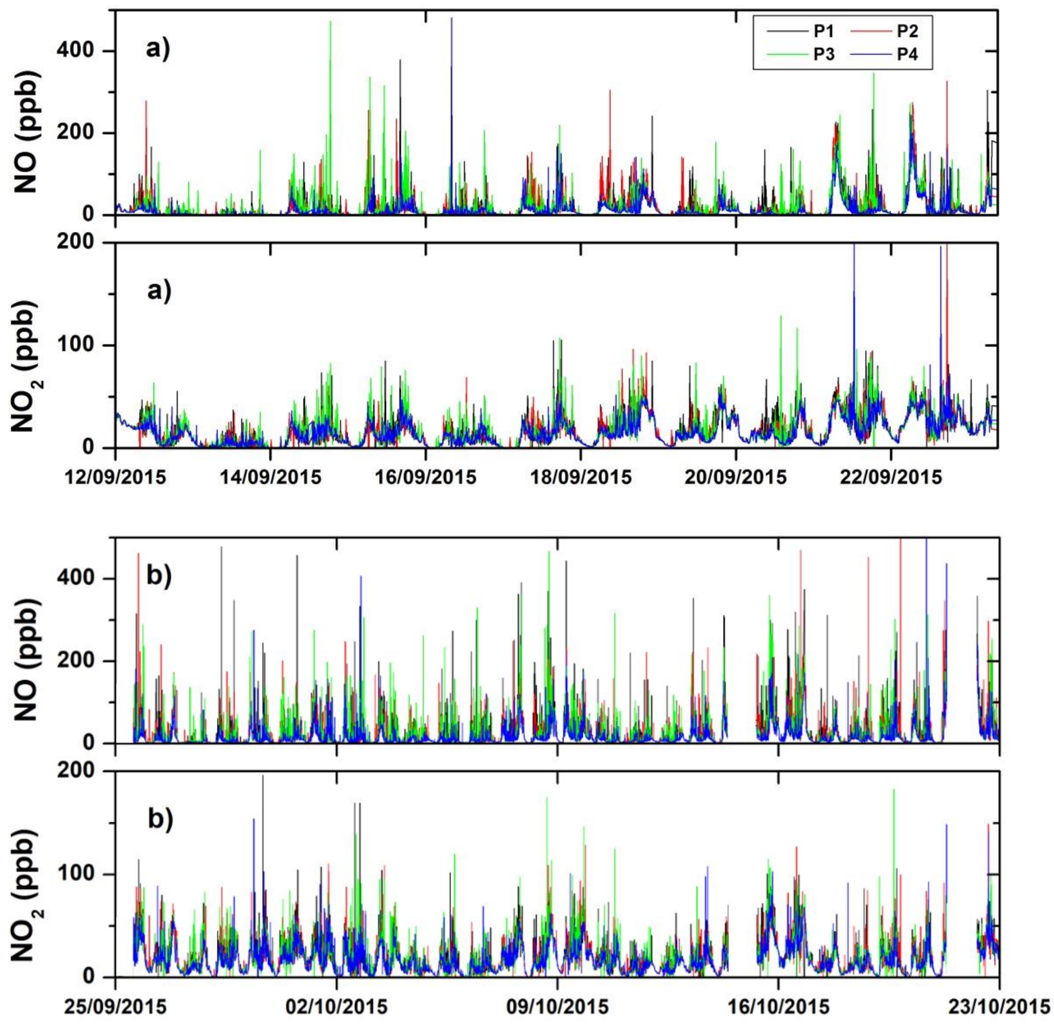


**Figure 5**. $NO_x$ concentrations along the road during the experimental campaign (12th September to 22nd October, 2015) registered at sampling locations P1 to P4, before (a) and after (b) the implementation of the photocatalytic coating on the road.

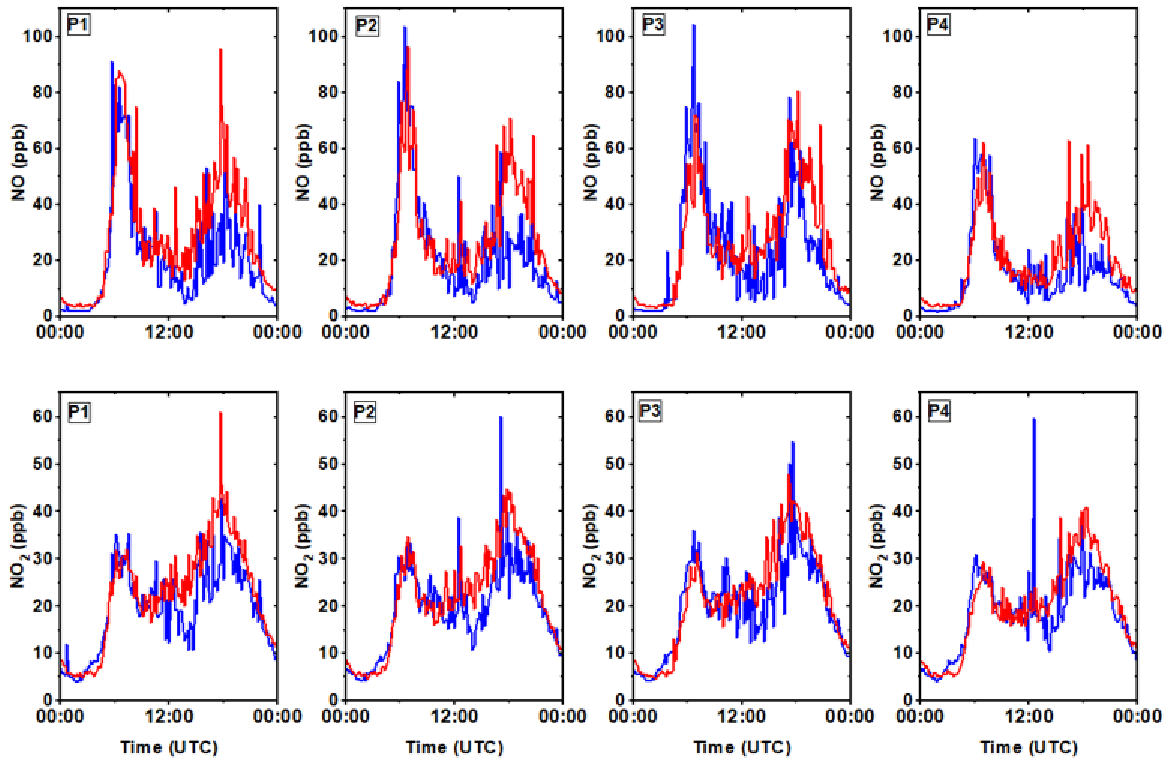


**Figure 6.** Daily mean profiles of 10-minutes averaged NO (upper) and $NO_2$ (lower) concentrations in P1 to P4 locations, before (blue line) and after (red line) the application of the photocatalytic coating on the bituminous pavement.

In addition, as shown in Figure 7, the daily mean concentrations of NO, $NO_2$ and $O_3$ registered at building's roof height (P7) throughout the campaign correspond to the typical behaviour of a suburban area mainly affected by traffic emissions produced in the nearby area.

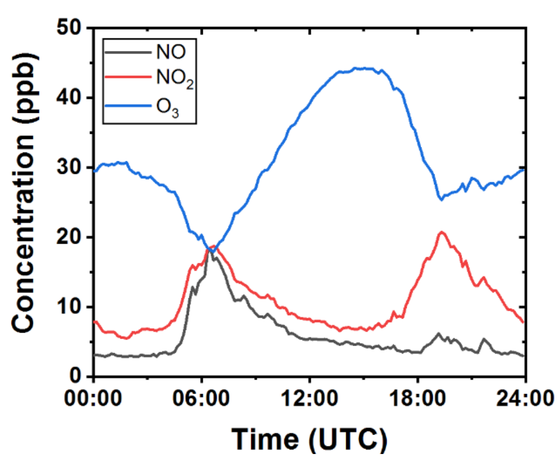


**Figure 7.** Daily mean profiles of 10-minutes averaged NO, $NO_2$ and $O_3$ concentrations in P7 location during the campaign.

Just as the NO concentrations recorded are mainly due to local emissions, the daily $NO_2$ profile reflects the additional contribution of its secondary generation through the oxidation of NO by $O_3$

present in the urban atmosphere. The daily evolution of NO, $NO_2$ and $O_3$ concentrations clearly reflects a typical ozone formation cycle influenced by both local emissions from the Alcobendas urban centre and those from the highways near the measurement point (P7) and the metropolitan area of Madrid, being the advection of these contaminated air masses and the consequent photochemical reactions the phenomena that modulate the generation of both $O_3$ and secondary $NO_2$ in the Madrid air basin (Plaza et al., 1997; Martín et al., 2001 a; Martín et al., 2001 b; Palacios et al., 2002).

Finally, near-road measurements of NO and $NO_2$ at P1 to P4 sites have allowed the estimation of daily averaged $NO_2/NO_x$ ratios, displayed in Figure 8, in which atmospheric chemistry also plays a determining role.

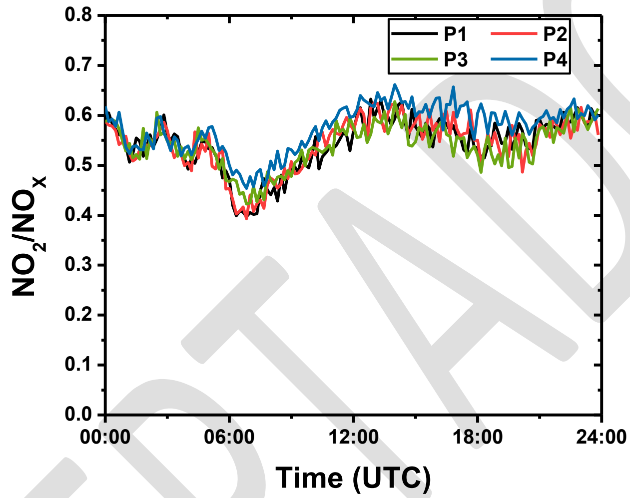


**Figure 8.** Daily mean profiles of $NO_2/NO_x$ ratios at P1 to P4 locations.

During late evening and overnight hours (21:00-06:00 UTC), typical atmospheric stable conditions and low traffic caused nocturnal $NO_2/NO_x$ profiles to be quite similar for all locations and values of around 0.55 were found. The 06:00–08:30 UTC period coincided with morning rush hours, when atmospheric conditions were transitioning to unstable and high traffic is established. Then a sharp decrease in $NO_2/NO_x$ ratios up to 0.4 levels can be noticed linked to vehicles exhaust emissions. Later, during the 08:30-18:00 UTC time period unstable conditions were established and a convective mixing together with moderate to high traffic emissions determined the observed ratio. A notable increase of $NO_2/NO_x$ up to 0.6 could be observed during the first hours of the period (until 14:00 UTC). After that, vehicle emissions started to increase again and a slight decrease in the ratios up to 0.5 when traffic intensity was maximum could be noticed. This behaviour is partially explained by the rapidly NO reaction with ambient ozone to form secondary $NO_2$, altering the on-road $NO_2/NO_x$ ratios that would be expected from tailpipe emissions alone. Finally, during late afternoon and early evening (18:00–21:00 UTC), atmospheric conditions were transitioning to stable and NO concentrations registered maxima levels at rush hour to approximately 10 ppb when traffic intensity markedly decreased. As a consequence, $NO_2/NO_x$ ratios varied from 0.4 to 0.6. The described behaviour is in accordance with results presented by other authors (Clements et al., 2009; Richmond-Bryant et al., 2017).

***Photocatalysis under optimal ambient conditions***

As it has been already demonstrated by a variety of laboratory experiments, the air depolluting capability of a photocatalytic material, depends not only on the active product itself and its photocatalytic properties, but also on several parameters as $NO_x$ mixing ratio, UV-A irradiance, relative humidity or flow rate [Devahasdin et al., 2003; Hüsken et al., 2009; Ballari et al., 2010; Hunger et al., 2010; Ballari et al., 2011; Martínez et al., 2011; Dillert et al., 2012; Ângelo et al., 2013; Sikkema et al., 2015; Toro et al., 2016; Mothes et al. 2018].

In this sense, modified-ISO tests performed on the selected material have shown how the variation in the imposed conditions causes the amount of NO removed from the gas phase by photocatalytic oxidation to be strongly affected by changes in light intensity, as well as by relative humidity. In point of fact, these tests have given as a result a reduction in the estimated surface deposition velocity when relative humidity increased from 20 to 65% to about one third, when the competition of the water molecules for the active sites in the photocatalytic surface makes difficult the adsorption of the pollutant, showing no significant photocatalytic activity when its humidity value reached 85%. Additionally, the activity was increasing by a factor of 2.5 when increasing the UV-A irradiance from 2 to 10 W $m^{-2}$ and remained constant at higher UV-A up to 40 W $m^{-2}$ [Palacios et al., 2015 e].

This dependence has also been observed in measurements of vertical $NO_x$ concentration gradients made in a suburban area [Palacios et al., 2015 d]. In this referred study photocatalytic activity was made evident only under specific meteorological conditions: relative humidity less than 63%, wind speed lower than 1.5 m $s^{-1}$ and solar irradiance higher than 400 W $m^{-2}$. A value of 3% of the irradiance can correspond to UV-A in the Madrid region [Escobedo et al., 2011]. Accordingly, a global irradiance value of 400 W $m^{-2}$ would correspond to UV-A radiation levels above 10 W $m^{-2}$.

Meteorological variables registered at building´s roof during the campaign have enabled characterizing the ambient conditions that could have an effect on the performance of the photocatalytic material put in place (Figure 9). In addition, these data supplied essential information for modelling purposes.

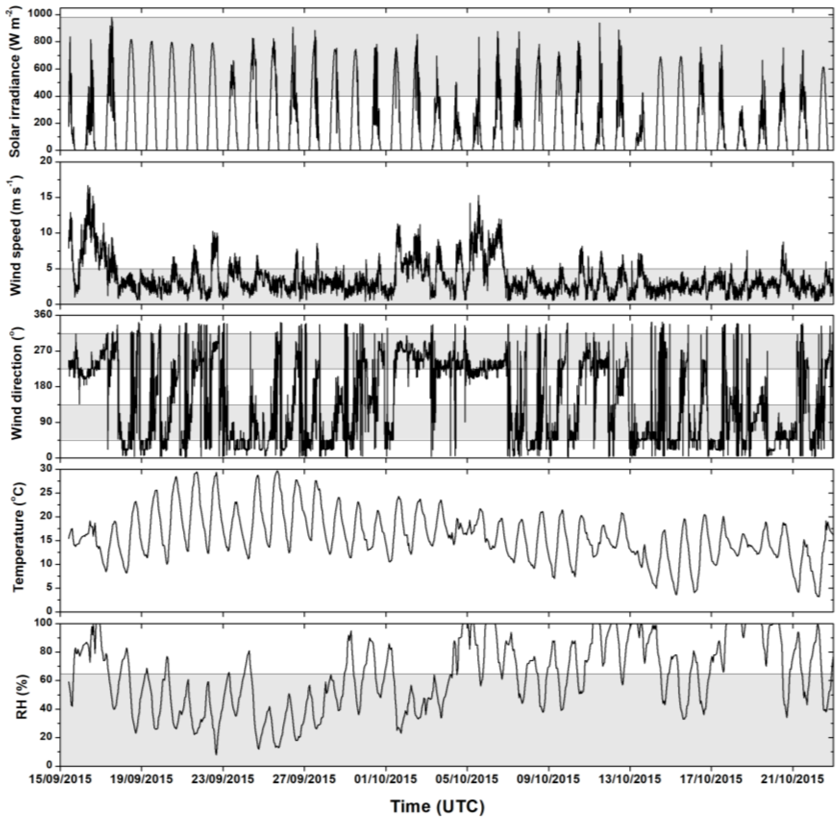


**Figure 9.** Meteorological variables registered at the roof of the Police building (P7) during the measurement campaign in the Paseo de la Chopera street. Ranges of parameters (solar irradiance, wind speed, wind direction and relative humidity) used for filtering experimental data are highlighted as shadow areas.

The analysis of the data was made taking into account above mentioned considerations. The meteorological conditions chosen to guarantee that $NO_x$ deposition rates could reach their maximum values on the photocatalytic pavement were the following: solar irradiance higher than 400 W $m^{-2}$, relative humidity less than 65% and wind speed lower than 5 m $s^{-1}$ (registered at 16 m height in P7 measurement point). Regarding the latest condition, in the 84% of these occasions, the surface wind speeds monitored in the near meteorological station of the Alcobendas municipality presented values less than 1.5 m $s^{-1}$. These favourable conditions have been registered during numerous periods along the measurement campaign.

In addition, the wind direction parameter was also included as a filtering condition in the analysis. Only wind directions close to the east-west direction were selected (sectors 45˚-135˚ and 225˚-315˚), favouring air flows almost parallel to the street (Figure 10). The simulations carried out with the micro-scale numerical model used in the course of the project made it possible to study the wind flows that develop in the street under different conditions, confirming the goodness of the ranges chosen for the filtering used (optimal ambient conditions) both for wind speeds and directions (Sanchez et al., 2016, 2017). This selection would allow capturing $NO_x$ gradients generated along the street axis that would be essentially associated with the presence of the photocatalytic surface and not with dynamic effects such as the formation of eddies that inherently induce strong concentrations gradients when complex air flows not parallel to the longitudinal axis of the street develop. There were very few data associated with the west sector that met all the conditions (1%), so the analysis was limited to the data for which the prevailing wind flow coming from the east sector that represented a 5% of the total data. The eastern flows show fairly similar frequencies of wind speeds. Therefore, the $NO_x$ gradients induced by the dynamics along the road will be predictably small and similar before and after the implementation of the photoactive material on the road. In this way, the differences that could be found between both situations could be attributed to a potentially remarkable photocatalytic effect.

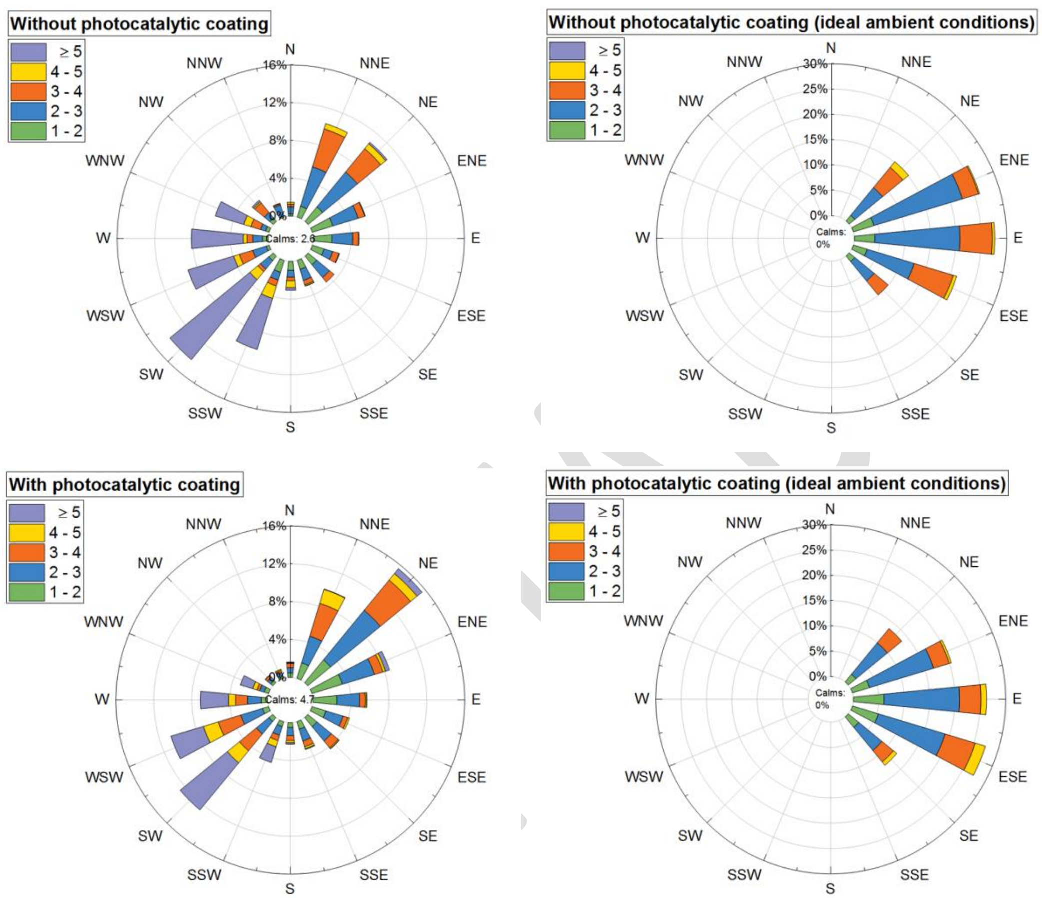


**Figure 10.** Wind roses summarizing the observations of the periods before and after the implementation of the photocatalytic material (left, all data; right, filtered data for optimal ambient conditions). The colour code represents the speed ranges in m $s^{-1}$.

The water adsorption and oxidation processes taking place on the photoactive surface are complex and depend on its hygroscopic state determined by the actual climatic-meteorological conditions (Baroghel-Bouny, 2007) that subsequently condition its photocatalytic reaction potential. Wetted surfaces (during/after rain or condensation events) become reduced or even nullified their $NO_x$ removal ability. Taking into account precipitation data from Alcobendas air quality station (Community of Madrid Network) and estimating dew temperature through relative humidity and temperature data from P7, data has been filtered to control the humidity of the substrate and the atmospheric humidity determining the photocatalytic reaction. Only periods for which two-day before the precipitation was zero and ambient temperature was higher than dew point were taken into account.

Concerning the span time of those events in which the environmental conditions were ideal for photocatalysis to be observed and their related frequency, only 7% of the cases presented a duration equal to or greater than one hour, while for 80% of them the persistence was less than 30 minutes (Figure 11).

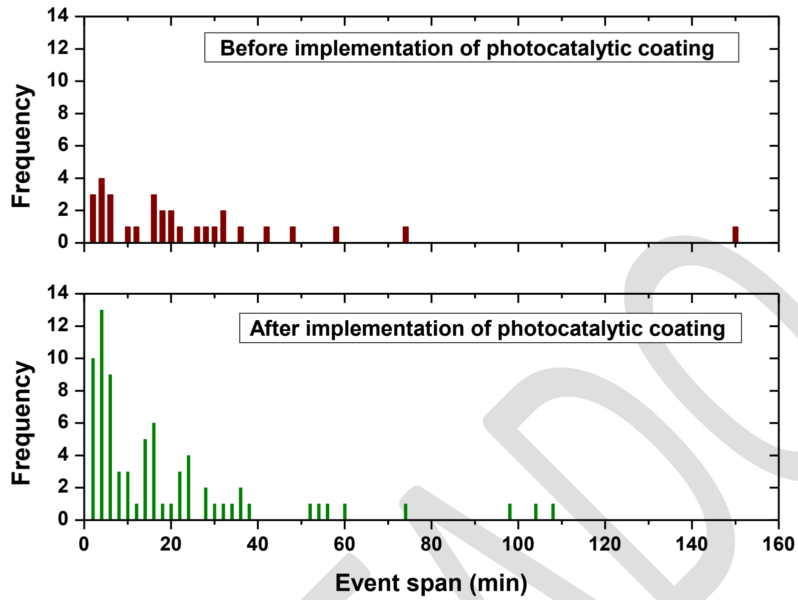


**Figure 11.** Event span and related frequency under selected optimal ambient conditions.

### *Assessment of $NO_x$ remediation*

As the sampling inlets of the experimental system in Paseo de la Chopera were arranged along the median strip of the road, one of the challenges to overcome in this research was to carefully preserve the chemical composition of air samples during the transportation time lapse along the sampling lines to the analyser, minimizing inside the tubing the possible partial evolution of NO by reactions with ozone or peroxy radicals.

No surface measurements of $O_3$ or volatile organic compounds were available at the time of the campaign. However, errors induced by the $NO/NO_2$ chemical conversion reactions have been avoided by analyzing the concentrations of $NO_x$.

As a result of the operating mode of the measuring system, $NO_x$ data were recorded every 8 minutes (measurement cycle) from each sampling point. In order to compare existing concentrations at sampling locations placed along the street at each time, the data associated with each point (P1 to P4) has been firstly interpolated to obtain a 2-minutes time-resolution series. Consequently, the same temporary basis has been applied to the meteorological data.

If the reduction of ambient $NO_x$ concentrations produced by the implementation of photocatalytic material on the road was significant, that is, if the environmental $NO_x$ concentration gradients of those pollutants along the road were higher than those induced by both local emissions and atmospheric dynamics and chemistry, the concentrations in the P2 and P3 locations should be clearly affected and clear decrease (taking P4 as reference) should be observed with respect to the situation previous to the photocatalytic material implementation. This approach, of course, starts from the premise that the scenario before the implementation of the photocatalytic material can be compared with that found after said treatment, since the physical morphology is the same and the environmental conditions in which it is compared (filtering data) and emissions are very similar.

In order to test the experimental system robustness, $NO_x$ concentrations registered at P1 to P4 locations during nocturnal periods (00:00-04:00 UTC) in the whole campaign have been processed to compute relevant statistics. Corresponding box charts are displayed in Figure 12. $NO_x$ means were 8.7, 8.9, 8.8 and 8.8 ppb for sites P1 to P4 and $NO_x$ variation coefficients (standard deviation/mean), used for comparing the degree of variation from one data series to another, were found to be of 62, 63, 62 and 64%, respectively. Therefore, a very similar behaviour along the experimental area was observed, as expected in stable night conditions and with very low road traffic, which confirms the correct performance of the measuring system and reveal the spatial homogeneity of the ambient $NO_x$ concentrations along the studied stretch in the absence of strong dynamic and near traffic emission perturbations.

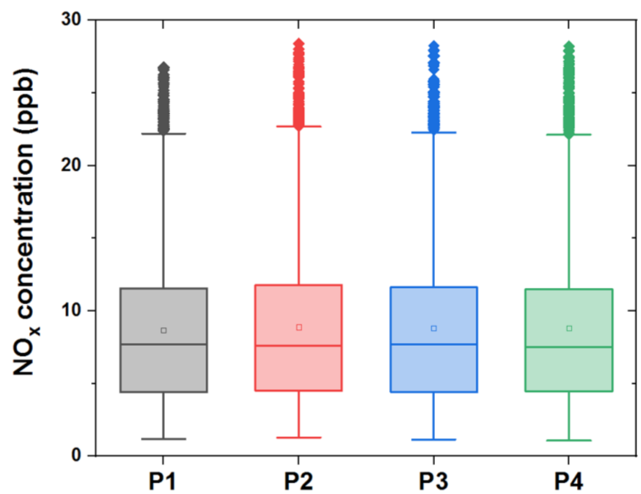


**Figure 12.** Box plots for $NO_x$ concentrations registered at P1 to P4 locations during the campaign for the 00:00-04:00 UTC period. Box: lower and upper limits are the 25$^{th}$ percentile (Q1) and the 75$^{th}$ percentile (Q3), respectively; median (line); mean (open symbol). Upper/lower bars: the largest/lower observed point from the dataset that falls within the distance of 1.5 times the interquartile range. All other observed points are plotted as outliers (diamond).

To evaluate the $NO_x$ reduction induced by the photoactive material of the roadway in the selected optimal ambient conditions, filtered data from measurement points P1 to P4 were processed to compare the behaviour of the control (without photocatalytic coating) and test (with photocatalytic coating) scenarios (Figure 13).

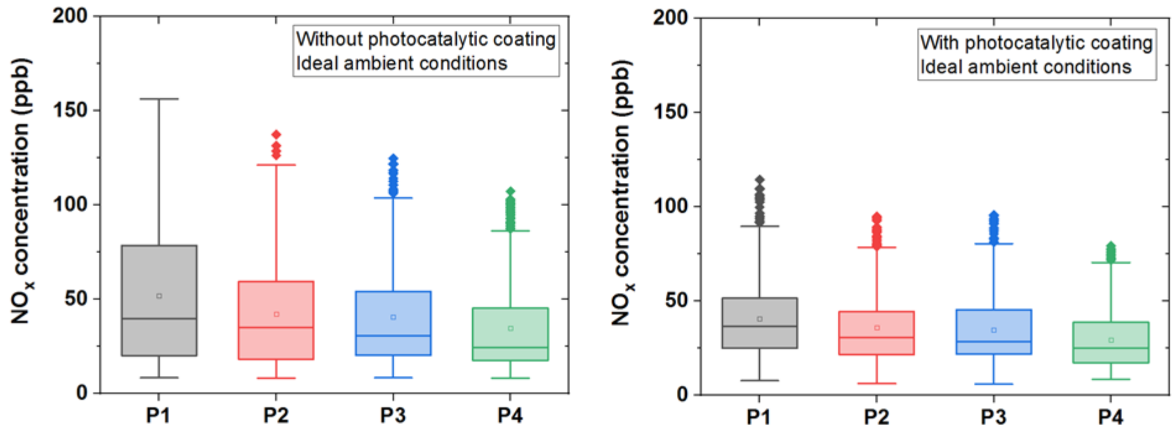


**Figure 13.** Box plots for $NO_x$ concentrations registered at P1 to P4 locations under optimal ambient conditions, before and after the implementation of the photocatalytic product. Box: lower and upper limits are the 25$^{th}$ percentile (Q1) and the 75$^{th}$ percentile (Q3), respectively; median (line); mean (open symbol). Upper/lower bars: the largest/lower observed point from the dataset that falls within the distance of 1.5 times the interquartile range. All other observed points are plotted as outliers (diamond).

The $NO_x$ mean concentrations at the different locations are significantly different and diverse between the studied periods despite they follow a similar trend. In principle, the chosen street has an optimal morphology to develop this research, that is, the experimental area is linear, without slopes and is a suitable street-canyon with the same type of buildings at both sides of the street. Furthermore, the data have been filtered in order to select a range of wind intensities and directions that minimizes the differential incidence that dynamic disturbances could have on the $NO_x$ gradients that are established along the street. However, even though practically all vehicles entering from the ends of the street (P5 and P6) pass through the experimental zone, the driving mode is obviously affected by the existing pedestrian crossings (P1 and P4), the perpendicular streets (P1) and the different circulation patterns through the different lanes that make up the road (existing parking areas attached to the sidewalks, specific parking of vehicles in the lanes of the roads, accesses to private car parks) (Figure 1). All these circumstances build a complex reality that translates into the already commented patent inhomogeneity of the $NO_x$ concentrations at the measurement locations (Table 2).

Having into account precision of ±0.4 ppb (500 ppb range) for the $NO_x$ analyzer measuring at sampling locations P1 to P4, the system would have been able to detect ambient $NO_x$ reductions related to a photocatalytic effect if they had been above 3%, in the average experimental conditions, within the range of 30 to 60 ppb.

**Table 2**. Statistics computed for $NO_x$ concentrations registered at P1 to P4 locations during optimal ambient conditions before and after the implementation of the photocatalytic product. Q1, 25$^{th}$ percentile and Q3, 75$^{th}$ percentile. (a) Nocturnal (00:00-04:00 UTC); (b) Control scenario (before); (c) Test scenario (after).

| | | N | Mean (ppb) | Standard deviation (ppb) | Coefficient of variation | Minimum (ppb) | Q1 (ppb) | Q3 (ppb) | Maximum (ppb) |
|---|---|---|---|---|---|---|---|---|---|
| (a) | $NO_x$ (P1) | 3932 | 8.7 | 5.3 | 0.6 | 1.2 | 4.4 | 11.6 | 26.8 |
| | $NO_x$ (P2) | 3932 | 8.9 | 5.6 | 0.6 | 1.3 | 4.5 | 11.8 | 28.4 |
| | $NO_x$ (P3) | 3932 | 8.8 | 5.5 | 0.6 | 1.1 | 4.4 | 11.6 | 28.3 |
| | $NO_x$ (P4) | 3932 | 8.8 | 5.6 | 0.6 | 1.1 | 4.4 | 11.5 | 28.2 |
| (b) | $NO_x$ (P1) | 390 | 51.8 | 36.8 | 0.7 | 8.4 | 20.1 | 78.6 | 156.4 |
| | $NO_x$ (P2) | 390 | 42.3 | 28.7 | 0.7 | 8.2 | 18.2 | 59.5 | 137.5 |
| | $NO_x$ (P3) | 390 | 40.6 | 27.0 | 0.7 | 8.3 | 20.2 | 54.1 | 124.7 |
| | $NO_x$ (P4) | 390 | 34.8 | 24.4 | 0.7 | 8.2 | 17.6 | 45.3 | 107.3 |
| (c) | $NO_x$ (P1) | 591 | 40.7 | 22.0 | 0.5 | 7.8 | 24.9 | 51.5 | 114.4 |
| | $NO_x$ (P2) | 591 | 36.0 | 19.5 | 0.5 | 6.2 | 21.6 | 44.4 | 94.9 |
| | $NO_x$ (P3) | 591 | 34.8 | 19.2 | 0.6 | 5.9 | 21.9 | 45.4 | 95.8 |
| | $NO_x$ (P4) | 591 | 29.5 | 15.6 | 0.5 | 8.5 | 17.2 | 38.7 | 79.2 |

Taking diurnal $NO_x$ concentrations registered at building's level (P7) before and after the application of the photocatalytic product under optimal ambient conditions, the ratio ($NO_x$ before/$NO_x$ after) showed an averaged ratio of 1.1 and could explain partially the difference between the mean concentrations found at street level. In the experimental area, the corresponding $NO_x$ ratios for P1 to P4 were 1.3, 1.2, 1.2 and 1.2, respectively, which reveals the influence of the urban background on the local $NO_x$ concentrations observed.

The difference in $NO_x$ concentrations found among the four measurement points prevents a direct comparison between the control and test scenarios. For this reason, keeping in mind the filtering ambient conditions applied to data set, the three measuring points potentially affected by the $NO_x$ sink effect were P1 to P3 and the differences in concentrations relative to the P4 location have been calculated. P4 has been taken as a reference point because this site is not subject to the influence of the photocatalytic effect under the east-wind sector selected.

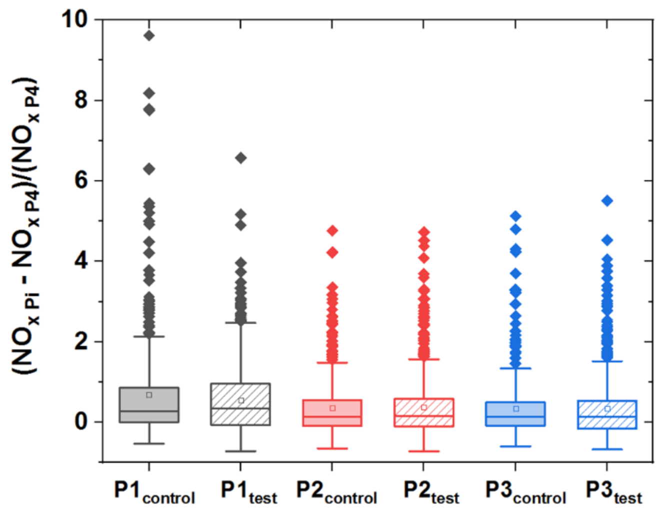


**Figure 14.** Relative $NO_x$ concentration differences for the control and test scenarios. Box: lower and upper limits are the 25th percentile (Q1) and the 75th percentile (Q3), respectively; median (line); mean (open symbol). Upper/lower bars: the largest/lower observed point from the dataset that falls within the distance of 1.5 times the interquartile range. All other observed points are plotted as outliers (diamond).

No variation in the relative $NO_x$ concentration differences (Figure 14) were found when test scenario is compared with the control one for P2 and P3 locations which implies that, even when a marked lessening is revealed at P1 (14%), no photocatalytic effect can be associated unequivocally to this ambient $NO_x$ reduction (see Table 3).

**Table 3.** Statistics computed for relative $NO_x$ concentrations differences registered at P1 to P4 locations during optimal ambient conditions before and after the implementation of the photocatalytic product. Q1, 25th percentile and Q3, 75th percentile. (a) Control scenario; (b) Test scenario.

| | Relative $NO_x$ differences | N | Mean (ppb) | Standard deviation (ppb) | Coefficient of variation | Minimum (ppb) | Q1 (ppb) | Q3 (ppb) | Maximum (ppb) |
|---|---|---|---|---|---|---|---|---|---|
| (a) | $(NO_{x\,P1}-NO_{x\,P4})/NO_{x\,P4}$ | 390 | 0.7 | 1.3 | 2.0 | -0.5 | 0.0 | 0.9 | 9.6 |
| | $(NO_{x\,P2}-NO_{x\,P4})/NO_{x\,P4}$ | 390 | 0.4 | 0.8 | 2.2 | -0.7 | -0.1 | 0.5 | 4.8 |
| | $(NO_{x\,P3}-NO_{x\,P4})/NO_{x\,P4}$ | 390 | 0.3 | 0.8 | 2.3 | -0.6 | -0.1 | 0.5 | 5.1 |
| (b) | $(NO_{x\,P1}-NO_{x\,P4})/NO_{x\,P4}$ | 591 | 0.6 | 0.9 | 1.6 | -0.7 | -0.1 | 1.0 | 6.6 |
| | $(NO_{x\,P2}-NO_{x\,P4})/NO_{x\,P4}$ | 591 | 0.4 | 0.8 | 2.2 | -0.7 | -0.1 | 0.6 | 4.7 |
| | $(NO_{x\,P3}-NO_{x\,P4})/NO_{x\,P4}$ | 591 | 0.3 | 0.8 | 2.5 | -0.7 | -0.2 | 0.5 | 5.5 |

Consequently, no macroscopic $NO_x$ sink effect due to the presence of the photocatalytic material implemented on the roadway could be unequivocally deduced under the studied experimental conditions.

Concerning the expected $NO_x$ removal in the urban ambient, upper limit photocatalytic $NO_x$ degradation was estimated in the experimental stretch of Paseo de la Chopera considering the street as an ideal street canyon [Ifang et al., 2014; Mothes et al., 2018]. The wind direction was considered so that the air mass stream flows at a constant velocity parallel to its longitudinal axis with no back mixing and an average wind speed was assumed to be 1.5 m $s^{-1}$. It was considered that air polluted mass is longitudinally transported through the canyon, without dilution to the upper air layer and traverses the 60 m long photocatalytic area. By taking the estimated NO surface deposition velocity for the selected photocatalytic material implemented on the road and considering $NO_2$ uptakes to be the same as those calculated for NO, a surface reactivity given by an $NO_x$ average deposition velocity of 7.2 $10^{-3}$ m $s^{-1}$ was assumed. This gives an $NO_x$ uptake coefficient of 7.8 $10^{-5}$. Considering the street-canyon cross section of 34 m × 16 m, an active surface to air volume above the surface ratio of 6 $10^{-2}$ $m^{-1}$ was then used to calculate a $NO_2$ first-order rate constant equal to 4.5 $10^{-4}$ $s^{-1}$. Taking the residence time of 40 s, the $NO_x$ degradation was then calculated, leading to a maximum estimated photocatalytic $NO_x$ potential remediation less than 2%, assuming bituminous pavement to be totally illuminated.

However, by using this simple approximation, no transport limitations are considered and only surface activity has been taken into account, neglecting turbulent mixing and quasi molecular-diffusion. If these latest were included, the real $NO_x$ uptake would decrease more than a factor of two [VDI 3782] ($NO_x$ remediation less than 1%). Moreover, surfaces are not active during night-time period and assuming half the daytime there is enough UV-A radiation for photocatalysis to take place, an average daily upper limit of approximately 0.5% is reached.

For a more accurate assessment, however, it is necessary to use a microscale model. The estimates made in the project with the CFD model evaluated in Paseo de la Chopera, is presented in the Part II manuscript (Sanchez et al., 2021).

**DISCUSSION**

Although laboratory studies on the photocatalytic material used in this urban scenario had clearly demonstrated its effectiveness for NO degradation (surface deposition velocity, 7.2 $10^{-3}$ m $s^{-1}$), from the results obtained during this field campaign no clear and direct causal relationship can be established between the presumed $NO_x$ depolluting capacity and the actual macroscopic environmental effect produced on immission levels when the photoactive material was implemented in the roadway. Other carefully designed field trials carried out in an artificial street canyon or an illuminated tunnel also failed to provide unquestionable evidences that tested photoactive materials used there caused a significant reduction in ambient $NO_x$ concentrations [Gallus et al., 2015 a, 2015 b].

The efficiency of any photoactive product applied on a surface in an open-air scenario and its actual effect on air quality depends firstly on the overall deposition velocity of the target pollutants on the photocatalytic surface but also on other determining environmental factors such as the temporal and spatial variability of near emissions, the very low photoactive surface/polluted atmospheric volume ratio, the complex geometry of the urban field site, etc. As a result, it is very difficult to establish experimentally the real depolluting effect in outdoor conditions of any photocatalytic material, but it is clear that the direct transfer of the nominal value of $NO_x$ depolluting capacity obtained from tests to real outdoor conditions should not be considered as a realistic or valid approach and real-scale experimental campaigns well designed are strongly recommended.

Although it has not been possible to identify any $NO_x$ sink effect that could be unequivocally related to the purifying action of the material implemented on the road, several reasons are excluded as a possible cause and are discussed below.

Most NO surface deposition velocity estimates in the related literature are equal or frequently lower than the values found for the present photoactive surface. In these conditions, when fast heterogeneous reactions are assumed, the transport of molecules to the surface is the limiting step the overall uptake process under typical street canyon conditions and average pollutant reductions of only a few percent have been estimated (<5%) [Bolte and Flassak, 2012; Boonen and Beeldens, 2014; Mothes et al., 2018; Gallus et al., 2015 b; Palacios et al., 2015 d; Laufs et al., 2010]. In this work, a calculation has been carried out following a first-order kinetic approach, according to which the $NO_x$ reductions expected in Paseo de la Chopera as a consequence of having implemented the selected photocatalytic product on the road would be less than 1%.

Moreover, as photocatalytic performance of the surface could be limited by ageing due to ambient conditions, wearing and soiling, the removal $NO_x$ capability of the material implemented on the road was periodically tested to evaluate its behaviour and to know if the coating needed any treatment to recover its best conditions. The extraction of the asphalt mix from the street was carried out during the measurement campaign and the NO photocatalytic activity was checked under ISO test, being able to observe that the photocatalytic activity was already less than half 25 days after applying the $TiO_2$-based coating.

The $NO_x$ concentrations recorded during the period selected as potentially active from a photocatalytic point of view should also be excluded as the cause of not having observed any sink effect, as long as average levels were in the range of 30 to 60 ppb, being 17 to 79 ppb for Q1-Q3 quartiles range.

For the material implemented on the bituminous pavement, NO conversion does not depend on atmospheric concentrations of this pollutant in experimental ambient conditions [Palacios et al., 2015 c; 2015 e] and NO degradation rate has been adjusted to a first order kinetics. Indeed, for such a mechanism, $NO_x$ conversion seems to be independent of the initial concentration even when the rates and the number of converted molecules has been observed to be proportional (Herrmann, 2010). However, other studies carried out at higher concentration values, for which order kinetics have not been defined as first order, defend that efficiencies might be influenced by the pollutant concentration revealing, eventually, lower abatements when pollutant levels increase (Devahasdin et al., 2003; Hüsken et al., 2009; Hunger et al., 2010; Martínez et al., 2011; Ângelo et al., 2013).

Furthermore, the experimental system implemented has allowed to compare concentration values simultaneously inside and outside the photoactive zone in a linear street in approximately identical ambient conditions, where the $NO_x$ analysers used were sensitive enough to quantify small absolute concentration differences.

Therefore, taking into account the enormous influence of environmental conditions such as wind speed and direction, humidity or solar irradiance on $NO_x$ removal efficiencies, analysis of these comprehensive collected data has allowed environmental situations to be considered for those that would be expected to have a greater $NO_x$ sink effect. Forcing the filtering of the data in order to select the most suitable ranges so that the direction and speed of the wind lead to the development of an air flow almost parallel to the axis of the street, would minimize the possibility of erroneously associating the $NO_x$ concentration gradients found with a potential photocatalytic sink effect when, actually, they would be simply induced by atmospheric dynamics. On the other hand, it is important to have in mind that higher turbulent mixing of the street-canyon air with the overlying atmosphere is expected for other non-selected wind directions, shortening the pollutants residence time and giving, consequently, less opportunity for the photocatalysis to take place.

But the greatest influence could be perhaps given from the large variations in ambient $NO_x$ concentrations, mainly due to emissions from traffic, with very high concentrations and frequency. In this sense, the bias that potentially be introduced by this interfering variable has also tried to be minimized in such a way that an analogous load and traffic pattern is assumed before and after the implementation of the photocatalytic material, based on the three intensive traffic registration campaigns during the measurement period. However, taking into account the behavior of a real street, this influence could be significant and potentially even greater than the photocatalytic effect that is intended to be observed.

Together with the data filtering procedure, the experimental design (high spatial and temporal resolution, an efficient distribution of the sampling points outside and inside the photoactive area, sampling inlets near the surface) has allowed to evaluate down in detail the behaviour of the air masses over the photocatalytic bituminous pavement and be aware of the enormous associated variability and characterize in sufficient detail the gradients established between the photoactive and non-photoactive zones. It is not surprising that the scenario does not behave as an ideal artificial street-canyon but as what it is, namely, a real street with a life of its own where the complex atmospheric dynamics, under unstable conditions, and the enormous influence of daytime local emissions are reflected in the different behaviour of the air masses at the different measurement points and gradients found among them. In contrast, at night, during stable conditions, it reveals very diverse from the daytime and with a minimal influence of the few existing local emissions, the four measurement points register similar concentrations. This diurnal inhomogeneity, which distances the operation of the studied system (street/urban atmosphere) from that which would take place in a reactor in which a laminar-plugged flow was established, is not surprising and is the typical situation in any real street.

The complexity of atmospheric phenomena involved should be considered when using basic statistics to evaluate real environmental data in order to infer any possible environmental effect derived from the use of photocatalytic materials in outdoor scenarios. Consequently, a basic condition to correctly quantify the $NO_x$ photocatalytic remediation has to be that similarity between reference and active areas are reasonable. If not, no homogeneous urban $NO_x$ background and different emission strength or pollutant dispersion conditions (geometry of the sites, sampling periods) may cause high uncertainties in the estimates. In the present study, reference and active areas are located one near each other and measurements have been taken under comparable decisive ambient conditions, minimizing the mentioned sources of error.

Very different removal efficiencies could be reported depending on the height at which pollutants are measured. Taking into account the small magnitude of the expected $NO_x$ deposition flows with respect to those of the actual emissions in the area, the design of the air sampling was conceived to allow the capture of the horizontal concentration changes near the photoactive surface, offering a higher probability of observing the possible impact of the existing sink effect caused by the induced downward $NO_x$ deposition fluxes. Obviously, at network stations (3 m high) it is not expected to detect a reduction greater than near the photocatalytic surface (Sanchez et al., 2021).

The ratio of photoactive surface to air volume above this surface ($S_{active}$/V ratio) for field trials in the open atmosphere has been defined as an important parameter limiting heterogeneous uptake and street canyon ratios of nearly 0.1 $m^{-1}$ are typical. The nonquantifiable $NO_x$ reductions found must not be explained by the geometry of the present canyon site which has a comparable Sactive/V ratio (0.06 $m^{-1}$) to other photocatalytic field experiments that reported higher $NO_x$ reduction (Guerrini and Peccati, 2007; Ballari and Brouwers, 2013). Other studies done under unrealistically high active surface to volume ratios (Maggos et al., 2008; Fraunhofer Institute for Molecular Biology and Applied Ecology IME, 2010) have shown also notable reductions but scaling down to real urban street conditions resulted in an estimated reduction of only ~5% (Laufs et al., 2010). Recently, PhotoPAQ project reported no significant photocatalytic remediation for $NO_x$, with only an upper limit of ≤ 2% under atmospheric conditions at an urban background site (Gallus et al., 2015 b). Similar results (4%) were found in the experimental system installed in a suburban area of Madrid (Germán et al., 2015).

Results extracted from data analysis have shown that horizontal relative $NO_x$ concentration differences found for both control and test scenarios have not allowed inferring any macroscopic photocatalytic effect on the air quality of the street due to the presence of the photocatalytic pavement. Moreover, the remarkable spatial variability observed in the concentrations along the street during the experimental campaign makes it extremely difficult to associate any reduction in $NO_x$ with an induced sink effect.

These findings do not imply that the photocatalytic phenomenon does not take place, but rather that its macroscopic effect on ambient $NO_x$ concentrations cannot be experimentally distinguished from the gradients induced by other atmospheric phenomena. In order to quantify the photocatalytic effects on ambient $NO_x$ concentrations in other conditions, microscale modelling, previously evaluated with experimental data from the conditions investigated in the present field study, is necessary (Part II) [Sanchez et al., 2021].

## CONCLUSIONS

In the present field study photocatalytic remediation of nitrogen oxides was studied in a real street of the municipality of Alcobendas (Community of Madrid, Spain) where a photocatalytic coating with a high $NO_x$ removal under laboratory standard test was applied on a bituminous pavement. A specific air quality measuring campaign was carried out during 41 days in early autumn, before and after the application of the coating on the road.

To tackle the experimental characterization of any expected pollution abatement due to the use of a photoactive surface in outdoor spaces, the design of the deployed experimental setup is critical and should complying with a series of fundamental specifications: active and reference areas with similar geometry and dispersive conditions and with a realistic active surface versus volume ratio, concentration measurements with high temporal and spatial resolution and quasi-simultaneous in both zones, parallel measurements of the variables meteorological influencing the photocatalytic process to characterize the behaviour of air masses in the street and, finally, air sampling inlets close enough to both the photoactive sinks and the reference non active surfaces. If not, any conclusion drawn about the ambient $NO_x$ depolluting strength of a surface may be easily misleading. Another key factor to ensure that any change in $NO_x$ concentrations can be related to the $TiO_2$-based surface and not to other factors is the careful selection of optimal ambient conditions in order to minimize the effect of interfering variables (dynamic and emissions) and facilitate the observation of the $NO_x$ sink.

Despite having carefully considered all the mentioned issues, no evident $NO_x$ remediation was observed in the street under the studied experimental conditions. Three main reasons explain it: the large polluted air volume compared to the active surface, the low estimated deposition fluxes of $NO_x$ when are compared to emission fluxes and the transport limitations of the pollutants towards the active surfaces typically existing at real open sites.

Microscale modelling can help to the estimation of the degree to which the environmental $NO_x$ reductions can be associated with the sink effect induced by the photocatalytic material because pollutant dispersion is simulated at high resolution taking into account the dispersive (wind fields, turbulence levels and pollutant transport and diffusion) and reactive (photochemistry) phenomenology of the atmosphere. Experimental data from this campaign have provided detailed relevant information that has allowed the evaluation of the performance of a computational fluid dynamic (CFD) model and its subsequent use to simulate the dispersive conditions and gradients of $NO_x$ concentrations in the street of Alcobendas in which the photocatalytic coating was applied (Part II of this manuscript). Both mentioned, experimental and numerical, methodologies, used in a complementary way, open up new possibilities for the air quality Administrations making its management feasible based on scientific results obtained in real urban environments in order to assess what role these photocatalytic materials could play within environmental quality policies and strategies for the public benefit.

**ACKNOWLEDGMENTS**

This study has been supported by LIFE MINO$_x$-STREET project (LIFE12 ENV/ES/000280) funded by European Commission. In addition, Alcobendas Council is thanked for the application of the photocatalytic coating and to enable the experimental deployment carried out in the area under study.

**REFERENCES**

Amorim, J.H., Rodrigues, V., Tavares, R., Valente, J., Borrego, C., 2013. CFD modelling of the aerodynamic effect of trees on urban air pollution dispersion. Sci. Total Environ. 461-462, 541–551. https://doi.org/10.1016/j.scitotenv.2013.05.031

Ângelo, J., Andrade, L., Madeira, L.M., Mendes, A., 2013. An overview of photocatalysis phenomena applied to $NO_x$ abatement. J. Environ. Manage. 129, 522–539. https://doi.org/10.1016/j.jenvman.2013.08.006

Ângelo, J., Andrade, L., Mendes, A., 2014. Highly active photocatalytic paint for $NO_x$ abatement under real-outdoor conditions. Appl. Catal. A Gen. 484, 17–25. https://doi.org/10.1016/j.apcata.2014.07.005

Ayuntamiento de Madrid, 2017. Plan A: Plan de Calidad del Aire y Cambio Climático de la Ciudad de Madrid. https://www.madrid.es/UnidadesDescentralizadas/Sostenibilidad/CalidadAire/Ficheros/PlanACalidadAire2019.pdf. (accessed in November 2020).

Ballari, M.M., Hunger, M., Hüsken, G., Brouwers, H.J.H., 2010. Modelling and experimental study of the $NO_x$ photocatalytic degradation employing concrete pavement with titanium dioxide. Catal. Today 151, 71–76. https://doi.org/10.1016/j.cattod.2010.03.042

Ballari, M.M., Yu, Q.L., Brouwers, H.J.H., 2011. Experimental study of the NO and $NO_2$ degradation by photocatalytically active concrete. Catal. Today 161, 175–180. https://doi.org/10.1016/j.cattod.2010.09.028

Ballari, M.M., Brouwers, H.J.H., 2013. Full scale demonstration of air-purifying pavement. J. Hazard. Mater. 254–255, 406–414. https://doi.org/10.1016/j.jhazmat.2013.02.012

Baroghel-Bouny, V., 2007. Water vapour sorption experiments on hardened cementitious materials: Part I: Essential tool for analysis of hygral behaviour and its relation to pore structure. Cem. Concr. Res. 37, 414–437. https://doi.org/10.1016/j.cemconres.2006.11.019

Beauchamp, M., Malherbe, L., de Fouquet, C., Létinois, L., 2018. A necessary distinction between spatial representativeness of an air quality monitoring station and the delimitation of exceedance areas. Environ. Monit. Assess. 190, 441. https://doi.org/10.1007/s10661-018-6788-y

Bengtsson, N., Castellote, M., 2010. Photocatalytic Activity for NO Degradation by Construction Materials: Parametric Study andMultivariable Correlations. J. Adv. Oxid. Technol. 13, 341–349. https://doi.org/10.1515/jaots-2010-0311

Bolte, G., Flassak, T., 2012. Numerische Simulation der Wirksamkeit photokatalytisch aktiver Betonoberflächen. In: Internationale Baustofftagung 18. ibausil (proceedings), Weimar, Germany, 1: 548-558. https://www.researchgate.net/publication/270898801_Numerische_Simulation_der_Wirksamkeit_photokatalytisch_aktiver_Betonoberflachen (accessed in November, 2020).

Boonen, E., Beeldens, A., 2014. Recent photocatalytic applications for air purification in Belgium. Coatings 4, 553–573. https://www.mdpi.com/2079-6412/4/3/553

Borge, R., Narros, A., Artiñano, B., Yagüe, C., Gomez-Moreno, F.J., de la Paz, D., RomanCascon, C., Díaz, E., Maqueda, G., Sastre, M., et al., 2016. Assessment of microscale spatio-temporal variation of air pollution at an urban hotspot in Madrid (Spain) through an extensive field campaign. Atmos. Environ. 140, 432–445. https://doi.org/10.1016/j.atmosenv.2016.06.020

Buccolieri, R., Salim, S.M., Leo, L.S., Di Sabatino, S., Chan, A., Ielpo, P., de Gennaro, G., Gromke, C., 2011. Analysis of local scale tree–atmosphere interaction on pollutant concentration in idealized street canyons and application to a real urban junction. Atmos. Environ. 45 (9), 1702–1713. https://doi.org/10.1016/j.atmosenv.2010.12.058

Cadavid, B., Sánchez de Juan, M., Marrón, J., Moral, A., Pérez, J., 2015. Participación del CEDEX dentro del proyecto LIFE $MINO_x$-Street. Revista Digital Del Cedex, (177), 13. http://193.145.71.12/index.php/ingenieria-civil/article/view/514 (accessed in November 2020).

Carslaw, D.C., Murrells, T.P., Andersson, J., Keenan, M., 2016. Have vehicle emissions of primary $NO_2$ peaked? Faraday Discuss. 189, 439–454. https://doi.org/10.1039/C5FD00162E

Chen, M., Chu, J.-W., 2011. $NO_x$ photocatalytic degradation on active concrete road surface-from experiment to real-scale application. J. Clean. Prod. 19, 1266–1272. https://doi.org/10.1016/j.jclepro.2011.03.001

Chen, H., Nanayakkara, C.E., Grassian, V.H., 2012. Titanium Dioxide Photocatalysis in Atmospheric Chemistry. Chem. Rev. 112, 5919–5948. https://doi.org/10.1021/cr3002092

Clements, A.L., Jia, Y., Denbleyker, A., McDonald-Bulle, E., Fraser, M.P., Allen, D.T., Collins, D.R., Michel, E., Pudota, J., Sullivan, D., Zhu, Y., 2009. Air pollutant concentrations near three Texas roadways, part II: Chemical characterization and transformation of pollutants. Atmos. Environ. 43, 4523–4534. https://doi.org/10.1016/j.atmosenv.2009.06.044

de Melo, J.V.S., Trichês, G., 2012. Evaluation of the influence of environmental conditions on the efficiency of photocatalytic coatings in the degradation of nitrogen oxides ($NO_x$). Build. Environ. 49, 117–123. https://doi.org/10.1016/j.buildenv.2011.09.016

Department for Environment Food and Rural Affairs (DEFRA), 2016. Paints and Surfaces for the Removal of Nitrogen Oxides. Report from Air Quality Expert Group to the Department for Environment Food and Rural Affairs. https://uk-air.defra.gov.uk/assets/documents/reports/cat11/1604130958_PB14425_Paints_and_Surfaces_for_the_Removal_of_Nitrogen_Oxides.pdf (accessed in November 2020).

Devahasdin, S., Fan, C., Li, K., Chen, D.H., 2003. $TiO_2$ photocatalytic oxidation of nitric oxide: transient behavior and reaction kinetics. J. Photochem. Photobiol. A Chem. 156, 161–170. https://doi.org/10.1016/S1010-6030(03)00005-4

Dillert, R., Stötzner, J., Engel, A., Bahnemann, D.W., 2012. Influence of inlet concentration and light intensity on the photocatalytic oxidation of nitrogen(II) oxide at the surface of Aeroxide® $TiO_2$

P25. J. Hazard. Mater. 211–212, 240–246. https://doi.org/10.1016/j.jhazmat.2011.11.041

Directive 2008/50/EC of the European Parliament and of the Council of 21 May 2008 on ambient air quality and cleaner air for Europe. https://eur-lex.europa.eu/legal-content/EN/TXT/PDF/?uri=CELEX:32008L0050&from=EN (accessed in November 2020).

European Committee for Standarization (ECS), 2012. Ambient air. Standard method for the measurement of the concentration of nitrogen dioxide and nitrogen monoxide by chemiluminiscence.

Engel, A., Glyk, A., Hülsewig, A., Große, J., Dillert, R., Bahnemann, D.W., 2015. Determination of the photocatalytic deposition velocity. Chem. Eng. J. 261, 88–94. https://doi.org/10.1016/j.cej.2014.03.040

Escobedo, J.F., Gomes, E.N., Oliveira, A.P., Soares, J., 2011. Ratios of UV, PAR and NIR components to global solar radiation measured at Botucatu site in Brazil. Renew. Energy 36, 169–178. https://doi.org/10.1016/j.renene.2010.06.018

European Environment Agency, 2019 a. Air quality in Europe — 2019 report, EEA Report No 10/2019. Luxembourg: Publications Office of the European Union. https://www.eea.europa.eu/publications/air-quality-in-europe-2019 (accessed in November 2020).

European Environment Agency, 2019 b. Air pollutant emissions data viewer (Gothenburg Protocol, LRTAP Convention) 1990-2018. https://www.eea.europa.eu/data-and-maps/dashboards/air-pollutant-emissions-data-viewer-3 (accessed in December 2020).

Fraunhofer Institute for Molecular Biology and Applied Ecology IME, 2010 Saubere Luft durch Pflastersteine/Clean air by Airclean®. Research activities 2009, 72-73. Fraunhofer Institute for Molecular Biology and Applied Ecology IME. https://www.ime.fraunhofer.de/content/dam/ime/de/documents/AE/2009_2010_Saubere%20Luft%20durch%20Pflastersteine_s.pdf (accessed in November 2020).

Gallus, M., Akylas, V., Barmpas, F., Beeldens, A., Boonen, E., Boréave, A., Cazaunau, M., Chen, H., Daële, V., Doussin, J.F., Dupart, Y., Gaimoz, C., George, C., Grosselin, B., Herrmann, H., Ifang, S., Kurtenbach, R., Maille, M., Mellouki, A., Miet, K., Mothes, F., Moussiopoulos, N., Poulain, L., Rabe, R., Zapf, P., Kleffmann, J., 2015 a. Photocatalytic de-pollution in the Leopold II tunnel in Brussels: $NO_x$ abatement results. Build. Environ. 84, 125–133. https://doi.org/10.1016/j.buildenv.2014.10.032

Gallus, M., Ciuraru, R., Mothes, F., Akylas, V., Barmpas, F., Beeldens, A., Bernard, F., Boonen, E., Boréave, A., Cazaunau, M., Charbonnel, N., Chen, H., Daële, V., Dupart, Y., Gaimoz, C., Grosselin, B., Herrmann, H., Ifang, S., Kurtenbach, R., Maille, M., Marjanovic, I., Michoud, V., Mellouki, A., Miet, K., Moussiopoulos, N., Poulain, L., Zapf, P., George, C., Doussin, J.F., Kleffmann, J., 2015 b. Photocatalytic abatement results from a model street canyon. Environ. Sci. Pollut. Res. 22, 18185–18196. https://doi.org/10.1007/s11356-015-4926-4

Germán, M., Palacios, M., Pujadas, M., Núñez, L., Fernández-Pampillón, J., 2015. Experimental study of $NO_x$ depolluting capabilities of a photocatalytic coating tested under suburban ambient conditions. 12th Urban Environment Symposium, Oslo, Norway, June 1-3. Extended abstract. http://www.lifeminoxstreet.com/life/showFile/87023ddf-8617-4000-b7a1-bd91c014b763/ (accessed in November 2020)

Gromke, C., Blocken, B., 2015. Influence of avenue-trees on air quality at the urban neighborhood scale. Part I: quality assurance studies and turbulent Schmidt number analysis for RANS CFD simulations. Environ. Pollut. 196, 214–223. https://doi.org/10.1016/j.envpol.2014.10.016

Guerrini, G.L., Peccati E., 2007. Photocatalytic Cementitious Roads for Depollution. In: International RILEM Symposium on Photocatalysis, Environment and Construction Materials, 179-186. Editor(s): P. Baglioni and L. Casssar. Print-ISBN: 978-2-35158-056-1. e-ISBN: 978-2-35158-057-

8. https://www.rilem.net/publication/publication/60?id_papier=7499

Hassan, M., Mohammad, L.N., Asadi, S., Dylla, H., Cooper, S., 2013. Sustainable Photocatalytic Asphalt Pavements for Mitigation of Nitrogen Oxide and Sulfur Dioxide Vehicle Emissions. J. Mater. Civ. Eng. 25, 365–371. https://doi.org/10.1061/(ASCE)MT.1943-5533.0000613

Herrmann, J.-M., 2010. Photocatalysis fundamentals revisited to avoid several misconceptions. Appl. Catal. B Environ. 99, 461–468. https://doi.org/10.1016/j.apcatb.2010.05.012

Hunger, M., Hüsken, G., Brouwers, H.J.H., 2010. Photocatalytic degradation of air pollutants — From modeling to large scale application. Cem. Concr. Res. 40, 313–320. https://doi.org/10.1016/j.cemconres.2009.09.013

Hüsken, G., Hunger, M., Brouwers, H.J.H., 2009. Experimental study of photocatalytic concrete products for air purification. Build. Environ. 44, 2463–2474. https://doi.org/10.1016/j.buildenv.2009.04.010

Ifang, S., Gallus, M., Liedtke, S., Kurtenbach, R., Wiesen, P., Kleffmann, J., 2014. Standardization methods for testing photo-catalytic air remediation materials: Problems and solution. Atmos. Environ. 91, 154–161. https://doi.org/10.1016/j.atmosenv.2014.04.001.

IPL, 2010. Improved Air Quality with Coating of Titanium Dioxide not Demonstrated, Dutch Air Quality Innovation Programme concluded, 16-17. http://laqm.defra.gov.uk/documents/Dutch_Air_Quality_Innovation_Programme.pdf (accessed in November 2020).

ISO, 2007. International standard ISO 22197-1:2007, 2007. Fine ceramics (advanced ceramics, advanced technical ceramics) -- Test method for air-purification performance of semiconducting photocatalytic materials -- Part 1: Removal of nitric oxide. https://www.iso.org/standard/40761.html

Jeanjean, A.P., Buccolieri, R., Eddy, J., Monks, P.S., Leigh, R.J., 2017. Air quality affected by trees in real street canyons: the case of Marylebone neighbourhood in Central London. Urban For. Urban Green. 22, 41–53. https://doi.org/10.1016/j.ufug.2017.01.009

Karapati, S., Giannakopoulou, T., Todorova, N., Boukos, N., Antiohos, S., Papageorgiou, D., Chaniotakis, E., Dimotikali, D., Trapalis, C., 2014. $TiO_2$ functionalization for efficient $NO_x$ removal in photoactive cement. Appl. Surf. Sci. 319, 29–36. https://doi.org/10.1016/j.apsusc.2014.07.162

Kurtenbach, R., Kleffmann, J., Niedojadlo, A., Wiesen, P., 2012. Primary $NO_2$ emissions and their impact on air quality in traffic environments in Germany. Environ. Sci. Eur. 24, 21. https://doi.org/10.1186/2190-4715-24-21

Laufs, S., Burgeth, G., Duttlinger, W., Kurtenbach, R., Maban, M., Thomas, C., Wiesen, P., Kleffmann, J., 2010. Conversion of nitrogen oxides on commercial photocatalytic dispersion paints. Atmos. Environ. 44, 2341–2349. https://doi.org/10.1016/j.atmosenv.2010.03.038

LIFE MINO$_x$-STREET, 2020. http://www.lifeminoxstreet.com/life (accessed in November 2020).

Maggos, T., Plassais, A., Bartzis, J.G., Vasilakos, C., Moussiopoulos, N., Bonafous, L., 2008. Photocatalytic degradation of $NO_x$ in a pilot street canyon configuration using $TiO_2$-mortar panels. Environ. Monit. Assess. 136, 35–44. https://doi.org/10.1007/s10661-007-9722-2

MAPAMA (Ministerio de Agricultura y Pesca, Alimentación y Medio Ambiente), 2017. Plan Nacional de Calidad del Aire 2017-2019 (Plan Aire II). https://www.miteco.gob.es/es/calidad-y-evaluacion-ambiental/temas/atmosfera-y-calidad-del-aire/planaire2017-2019_tcm30-436347.pdf (accessed in November 2020).

Martín, F., Crespí, S.N., Palacios, M., 2001 a. Simulations of mesoscale circulations in the center of the Iberian Peninsula for thermal low pressure conditions. Part I: Evaluation of the topography vorticity-mode mesoscale model. J. Appl. Meteorol. 40 (5), 880-904. https://doi.org/10.1175/1520-0450(2001)040%3C0880:SOMCIT%3E2.0.CO;2

Martín, F., Palacios, M., Crespí, S.N., 2001 b. Simulations of mesoscale circulations in the center of the Iberian Peninsula for thermal low pressure conditions. Part II: Air-parcel transport patterns. J. Appl. Meteorol. 40 (5), 905-914. https://doi.org/10.1175/1520-0450(2001)040%3C0905:SOMCIT%3E2.0.CO;2

Martínez, T., Bertron, A., Ringot, E., Escadeillas, G., 2011. Degradation of NO using photocatalytic coatings applied to different substrates. Build. Environ. 46, 1808–1816. https://doi.org/10.1016/j.buildenv.2011.03.001

Mendoza, C., Valle, A., Castellote, M., Bahamonde, A., Faraldos, M., 2015. $TiO_2$ and $TiO_2$–$SiO_2$ coated cement: Comparison of mechanic and photocatalytic properties. Appl. Catal. B Environ. 178, 155–164. https://doi.org/10.1016/j.apcatb.2014.09.079

Mothes, F., Ifang, S., Gallus, M., Golly, B., Boréave, A., Kurtenbach, R., Kleffmann, J., George, C., Herrmann, H., 2018. Bed flow photoreactor experiments to assess the photocatalytic nitrogen oxides abatement under simulated atmospheric conditions. Appl. Catal. B Environ. 231. https://doi.org/10.1016/j.apcatb.2018.03.010

Núñez, L., Palacios, M., Pujadas, M., Fernández-Pampillón, J., Gómez-Mancebo, M. B., Fernández, M., Mazario, A., Suárez, S., Sánchez, B., 2018. Study of the effects on airborne and lixiviates due to the wear of a photocatalytic product applied outdoors. Proceedings of abstracts of the 11th International Conference on Air Quality - Science and Application, 181. Barcelona, Spain March 12-16, 2018. Editors: Ranjeet S. Sokhi, María José Gállego, Pushp Raj Tiwari, Joan Marc Craviotto Arnau, Cristina Castells Guiu, Vikas Singh. doi: 10.18745/PB.19829. https://uhra.herts.ac.uk/bitstream/handle/2299/19829/AQ_Proceedings_2018.pdf?sequence=3&isAllowed=y

Palacios, M., Kirchner, F., Martilli, A., Clappier, A., Martín, F., Rodríguez, M.E., 2002. Summer ozone episodes in the Greater Madrid Area. Analyzing the ozone response to abatement strategies by modelling. Atmos. Environ. 36-34, 5323-5333. https://doi.org/10.1016/S1352-2310(02)00590-3

Palacios, M., Núñez, L., Pujadas, M., Suárez, S., Sánchez, B., Gómez-Mancebo, M.B., Fernández-Pampillón, J., Mazarío-Fernández, A., Moral, A., Pérez, J., 2015 a. Durability of a photocatalytic coating on a bituminous pavement. Proceedings of the International Conference on Sustainable Materials and Science Technology, 213. Paris, France, July 15-17, 2015. ISBN: 978-84-944311-0-4. Edited by: ScienceKNOW Conferences C.B. Available at http://www.lifeminoxstreet.com/life/showFile/a48082a9-188d-4a30-bd85-1121c50797b4/ (accesed in November, 2020).

Palacios, M., Núñez, L., Suárez, S., Sánchez, B., Pujadas, M., Fernández-Pampillón, J., 2015 b. Selection of commercial photocatalytic materials based on their air-purifying ability. Proceedings of the International Conference on Sustainable Materials and Science Technology, 231. Paris, France, July 15-17, 2015. ISBN: 978-84-944311-0-4. Edited by: ScienceKNOW Conferences C.B. Available at http://www.lifeminoxstreet.com/life/showFile/08e14d80-1afa-41f0-a18c-856ee4ecdb4b/ (accessed in November, 2020).

Palacios, M., Suárez, S., Núñez, L., Sánchez, B., Pujadas, M., Fernández-Pampillón, J., 2015 c. $NO_x$ photocatalytic degradation employing concrete surfaces with titanium dioxide. Proceedings of the International Conference on Chemical and Biochemical Engineering, 258. Paris, France, July 20-22, 2015. ISBN: 978-84-944311-1-1. Edited by: ScienceKNOW Conferences C.B. Available at http://www.lifeminoxstreet.com/life/showFile/79df9071-4a94-4a2e-aecd-edb9e1b63b8a/ (accessed in November, 2020).

Palacios, M., Núñez, L., Pujadas, M., Fernández-Pampillón, J., Germán, M., Sanchez, B., Santiago, J.L., Martilli, A., Suárez, S., Cabrero, B.S., 2015 d. Estimation of $NO_x$ deposition velocities for selected commercial photocatalytic products. Twenty-third International Conference on

Modelling, Monitoring and Management of Air Pollution, Air Pollution XXIII. Transaction WIT Transactions on The Built Environment, 168, 729 – 740. doi. 10.2495/SD150642. https://www.witpress.com/elibrary/wit-transactions-on-the-built-environment/168/34810

Palacios, M., Suárez, S., Núñez, L., Sánchez, B., Pujadas, M., Fernández-Pampillón, J., 2015 e. Influence of parameters on the photocatalytic oxidation of nitric oxide at the surface of titanium dioxide-modified concrete materials. Proceedings of the International Conference on Chemical and Biochemical Engineering, 294. Paris, France, July 20-22, 2015. ISBN: 978-84-944311-1-1. Edited by: ScienceKNOW Conferences C.B. Available at http://www.lifeminoxstreet.com/life/showFile/fe760e83-8b86-4141-b527-a268939afa0c/ (accessed in November, 2020).

Plaza, J., Pujadas, M., Artíñano, B., 1997. Formation and Transport of the Madrid Ozone Plume, Journal of the Air & Waste Management Association, 47:7, 766-774. https://doi.org/10.1080/10473289.1997.10463938

Richmond-Bryant, J., Owen, R. C., Graham, S., Snyder, M., McDow, S., Oakes, M., Kimbrough, S., 2017. Estimation of on-road $NO_2$ concentrations, $NO_2/NO_x$ ratios, and related roadway gradients from near-road monitoring data. Air. Qual. Atmos. Health. 10, 611–625. https://doi.org/10.1007/s11869-016-0455-7

Rivas, E., Santiago, J.L., Lechón, Y., Martín, F., Ariño, A., Pons, J.J., Santamaría, J.M., 2019. CFD modelling of air quality in Pamplona City (Spain): assessment, stations spatial representativeness and health impacts valuation. Sci. Total Environ. 649, 1362–1380. https://doi.org/10.1016/j.scitotenv.2018.08.315

Samoli, E., Aga, E., Touloumi, G., Nisiotis, K., Forsberg, B., Lefranc, A., Pekkanen, J., Wojtyniak, B., Schindler, C., Niciu, E., Brunstein, R., Dodič Fikfak, M., Schwartz, J., Katsouyanni, K., 2006. Short-term effects of nitrogen dioxide on mortality: an analysis within the APHEA project. Eur. Respir. J. 27, 1129 LP – 1138. https://doi.org/10.1183/09031936.06.00143905.

Sanchez, B., Santiago, J.L., Martilli, A., Palacios, M., Pujadas, M., Núñez, L., Germán, M., Fernandez-Pampillón, J., Iglesias, J.D., 2016. CFD Modeling of Reactive Pollutants Dispersion and Effect of Photocatalytic Pavements in a Real Urban Area. Oral presentation on 17th International Conference on Harmonisation within Atmospheric Dispersion Modelling for Regulatory Purposes, Budapest, Hungary. http://www.harmo.org/conferences/Proceedings/_Budapest/publishedSections/PPT/H17-103_oral.pdf (accessed in November 2020).

Sanchez, B., Santiago, J.L., Martilli, A., Martin, F., Borge, R., Quaassdorff, C., de la Paz, D., 2017. Modelling $NO_x$ concentrations through CFD-RANS in an urban hot-spot using high resolution traffic emissions and meteorology from a mesoscale model. Atmos. Environ. 163, 155–165. https://doi.org/10.1016/j.atmosenv.2017.05.022

Sanchez, B., Santiago, J.L., Martilli, A., Palacios, M., Núñez, L., Pujadas, M., Fernández-Pampillón, J., 2021. $NO_x$ Depolluting Performance of Photocatalytic Materials in anUrban Area - Part II: Assessment through Computational Fluid Dynamics Simulations. Atmos. Environ. 246, 118091. https://doi.org/10.1016/j.atmosenv.2020.118091

Sánchez, B., Suárez, S., Jansson, I., Vilanova, O., Martínez, C., 2014. First results of the LIFE $MINO_x$-STREET project: Monitoring and modelling $NO_x$ removal efficiency of commercial photocatalytic materials. International Conference Photocatalysis Standardization and Certification Assisting Commercialization. Prague, Czech Republic, September 03-04, 2014. http://www.lifeminoxstreet.com/life/showFile/36f3de55-bed6-4c22-9be9-ea2146d1699f/ (accessed in November 2020).

Sánchez, B., Suárez, S., Jansson, I., Vilanova, O., Cadavid, B., Perez, J., Marrón, J.O., Moral, A., Sánchez, M., Palacios, M., Núñez, L., Artiñano, B., Pujadas, M., Iglesias, D., 2015. Assessment of the key parameters of the photocatalytic properties for construction materials: LIFE-MINO$_x$-STREET, European Project. Proceedings of the 4th European Conference on Environmental Applications of Advanced Oxidation Processes, Páginas Athens, Greece, October 21-24, 2015. http://www.lifeminoxstreet.com/life/showFile/f4cdf8aa-3707-44fa-9f4b-f6ef78fda667/ (accessed in November 2020).

Santiago, J.L., Borge, R., Martín, F., de la Paz, D., Martilli, A., Lumbreras, J., Sanchez, B., 2017. Evaluation of a CFD-based approach to estimate pollutant distribution within a real urban canopy by means of passive samplers. Sci. Total Environ. 576, 46–58. https://doi.org/10.1016/j.scitotenv.2016.09.234

Santiago, J.L., Sanchez, B., Quaassdorff, C., de la Paz, D., Martilli, A., Martín, F., Borge, R., Rivas, E., Gómez-Moreno, F.J., Díaz, E., Artiñano, B., Yagüe, C., Vardoulakis, S., 2020. Performance evaluation of a multiscale modelling system applied to particulate matter dispersion in a real traffic hot spot in Madrid (Spain). Atmos. Pollut. Res. 11 (1), 141–155. https://doi.org/10.1016/j.apr.2019.10.001

Sikkema, J.K., Ong, S.K., Alleman, J.E., 2015. Photocatalytic concrete pavements: Laboratory investigation of NO oxidation rate under varied environmental conditions. Constr. Build. Mater. 100, 305–314. https://doi.org/10.1016/j.conbuildmat.2015.10.005

Suárez, S., Martínez, C., Vilanova, O., Sánchez, B., 2017. Commercial photocatalytic products to reduce NO$_x$ pollution from cities: from lab to urban asphalt. 4th Photocatalytic and Superhydrophilic Surfaces Workshop. Manchester, United Kingdom, December 07-08, 2017. http://www.lifeminoxstreet.com/life/events/congresses/detail/;jsessionid=102D5F4D966BB1DB4F78F52E8EB82799.nodo2?uuid=9c8caf0d-088a-47b7-ae02-66f00c0eb196 (accessed in November 2020).

Toro, C., Jobson, B.T., Haselbach, L., Shen, S., Chung, S.H., 2016. Photoactive roadways: Determination of CO, NO and VOC uptake coefficients and photolabile side product yields on TiO2 treated asphalt and concrete. Atmos. Environ. 139, 37–45. https://doi.org/10.1016/j.atmosenv.2016.05.007

Tremper, A., Green, D., 2016. Artworks D-NO$_X$ Paint Trial Report. King's College London. https://www.southwark.gov.uk/assets/attach/2407/Artworks_PainTrial_Report_final.pdf (accessed in November, 2020).

United Nations, DESA/Population Division, 2018. World Urbanization Prospects 2018. https://population.un.org/wup/Download/ (accessed in November 2020).

Vardoulakis, S., Fisher, B.E., Pericleous, K., Gonzalez-Flesca, N., 2003. Modelling air quality in street canyons: a review. Atmos. Environ. 37 (2), 155–182. https://doi.org/10.1016/S1352-2310(02)00857-9

Vardoulakis, S., Solazzo, E., Lumbreras, J., 2011 a. Intra-urban and street scale variability of BTEX, $NO_2$ and $O_3$ in Birmingham, UK: implications for exposure assessment. Atmos. Environ. 45 (29), 5069–5078. https://doi.org/10.1016/j.atmosenv.2011.06.038

Vardoulakis, S., Dimitrova, R., Richards, K., Hamlyn, D., Camilleri, G., Weeks, M., Sini, J.-F., Britter, R., Borrego, C., Schatzmann, M., Moussiopoulos, N., 2011 b. Numerical model inter-comparison for wind flow and turbulence around single-block buildings. Environ. Model. Assess. 16 (2), 169–181. https://doi.org/10.1007/s10666-010-9236-0

VDI (Verein Deutscher Ingenieure), 2006. VDI 3782, Part 5. Environmental Meteorology, Atmospheric Dispersion Models, Deposition Parameters, VDI/DIN-Handbuch Reinhaltung der Luft, Band 1b.

Villena, G., Bejan, I., Kurtenbach, R., Wiesen, P., Kleffmann, J., 2012. Interferences of commercial $NO_2$ instruments in the urban atmosphere and in a smog chamber. Atmos. Meas. Tech. 5, 149–159. https://doi.org/10.5194/amt-5-149-2012

Vos, P.E., Maiheu, B., Vankerkom, J., Janssen, S., 2013. Improving local air in cities: to tree or not to tree? Environ. Pollut. 183, 113–122. https://doi.org/10.1016/j.envpol.2012.10.021

WHO Regional Office for Europe, 2013. Review of evidence on health aspects of air pollution-REVIHAAP Project. Technical Report. https://www.euro.who.int/__data/assets/pdf_file/0004/193108/REVIHAAP-Final-technical-report-final-version.pdf (accessed in November 2020).

WHO Regional Office for Europe, 2017. Evolution of WHO air quality guidelines: past, present and future. https://www.euro.who.int/__data/assets/pdf_file/0019/331660/Evolution-air-quality.pdf (accessed in November 2020).

Zouzelka, R., Rathousky, J., 2017. Photocatalytic abatement of $NO_x$ pollutants in the air using commercial functional coating with porous morphology. Appl. Catal. B Environ. 217, 466–476. https://doi.org/10.1016/j.apcatb.2017.06.009